

# 7 DESCRIBING FUNCTIONS FOR NONLINEAR SYSTEMS WITH RANDOM INPUTS

## 7.0 INTRODUCTION

The preceding chapters have dealt with approximate descriptions of nonlinearities having inputs consisting of the sums of two commonly considered signal forms, sinusoids and constants. We wish now to add a third form to this repertory of input signals, a random process. The study of nonlinear systems with random inputs is of consequence both because the design of many high-performance systems is significantly influenced by the presence of undesired random noise and because the signal inputs expected in many operational circumstances do not permit description in deterministic terms. Realistic input signals often can be characterized only as members of an ensemble of possible input functions, the ensemble having certain statistical properties which are known or can be estimated.

Actually, the general theory of describing functions developed in Chap. 1 was couched in statistical terms at the outset. This was done so most signal forms of interest at the nonlinearity input could be included in a single format. To this end, sinusoidal and bias signals have been treated as special

cases of random processes. This led to describing functions for these signals which have the more familiar interpretation in terms of harmonic analysis.

In this chapter we consider, in addition to constants and sinusoids, random signals of the ordinary sort which do not have characteristic waveshapes. In this case a statistical approach is clearly essential, and no alternative deterministic interpretation seems possible. There is a considerable literature on the subject of quasi-linearization of nonlinear elements driven by random signals. Much of this is related to random signals having finite power density spectra, which rules out consideration of biases and sinusoids. This literature is briefly reviewed in the following section, after which the calculation and application of describing functions for systems with random inputs is discussed. A review of probability theory, random variables, and random processes appears in Appendix H for convenient reference.

## 7.1 STATISTICAL LINEARIZATION

A time-honored procedure for dealing in a practical way with nonlinear systems is to construct a linear model to approximate the nonlinearities. Thus, for example, a small-signal linearization consists of expanding the nonlinear function in a Taylor series about some operating point and retaining only the linear terms in the analysis. If the signals at the input to the nonlinearity are not small enough to permit this simple form of linearization, one can do better by allowing the linear approximator to depend on the input. A linear operator whose parameters depend on certain static characteristics of the input is referred to as *quasi-linear*. Quasi-linearization can be accomplished only if the form of the signal at the input to the nonlinearity is assumed in advance. The assumption of a *sinusoidal signal* leads to the ordinary describing function; that analysis is appropriately referred to as *harmonic linearization*.

Similarly, if we deal with nonlinear systems having *random inputs* by use of quasi-linear approximators to the nonlinearities, we refer to the procedure as *statistical linearization*. There is a variety of ways in which such an approximation may be formed. The quasi-linear approximator cannot model all the input-output transfer characteristics of the nonlinearity; so one must choose which of these characteristics to use as the basis for definition of the approximator. This choice does not seem as evident in the case of the random input as it did with a sinusoidal input.

If the nonlinearity is of dynamic character, a dynamic linear operator must somehow be defined as the approximator. If the nonlinearity is static, one is strongly tempted to approximate it with a static linear operator—a gain. As reasonable as this sounds, it still represents a somewhat arbitrary choice. One of the most important statistical characteristics of the output of the

nonlinearity with a random input, its power spectral density function (or equivalently, its autocorrelation function), cannot be duplicated at the output of the approximating operator if it is just a gain. If the assumption is made that the random process at the input to the nonlinearity is gaussian, the autocorrelation function of the output can readily be expressed as a power series in the input autocorrelation function as in Eq. (H-77). The Fourier transform of this autocorrelation function is the power density spectrum of the output of the nonlinearity, and the ratio of this function to the input power density spectrum defines the square of the magnitude of a transfer function which can be taken as a dynamic linear approximation to the static nonlinearity. The virtue of this approximation is that it produces a power density spectrum at its output equal to that of the nonlinearity it approximates. Several authors have employed this method of quasi-linearization. Pupkov (Ref. 36) gives in graphical form the first five coefficients,  $a_k$ , required for the series expansion of the output autocorrelation function for several common nonlinearities. Culver and Mesarovic (Ref. 10) suggest this procedure as a practical alternative to a still more general, but much more complicated, method of dynamic linearization. Kazakov (Ref. 18) summarizes the conditions which define two dynamic linear operators to approximate a static nonlinearity, one to operate on the mean and the other on the random component of the input, so as to match at their outputs the mean value and autocorrelation function of the output of the nonlinearity. He states, however, that investigations by a number of authors have not conclusively shown that the performance of closed-loop systems which include a static nonlinearity is better predicted by the use of a dynamic, as opposed to a static, linear approximation to the nonlinearity. Caron (Ref. 8) has taken a different approach to the end of matching the autocorrelation functions at the outputs of the nonlinearity and its approximator. He employs as his quasi-linear model of the nonlinearity a static gain chosen to equate the input-output cross-correlation functions for model and nonlinearity, to the output of which he adds a random signal calculated to equate the autocorrelation functions. In the application of this procedure, however, he predicts signals that have negative values for their power spectral density functions over portions of the frequency range. This physically meaningless result remains unexplained.

Actually, the distinction between a static and dynamic quasi-linear approximator for a static nonlinearity is probably of lesser consequence to the accuracy of the representation of a nonlinear feedback system than the assumption which is common to both—that the random process at the input to the nonlinearity is gaussian. This assumption seems essential to permit a practicable attack on all but the simplest of problems. The procedure required to calculate, rather than assume, the distribution of amplitudes at the input to the nonlinearity is described and illustrated by

Chuang and Kazda (Ref. 9). For systems of higher order than second, their approach can be pursued to its conclusion only in special cases, and in these cases the procedure is complicated enough to defy the interpretation and understanding of results which are essential to the system designer. We are left, then, with the necessity of assuming the form of the distribution function for the nonlinearity input; clearly, the only cases in which this can be done are those in which the input to the system is gaussian, and the nature of the feedback system is such that the input to the nonlinearity can also be assumed gaussian. The situations in which this assumption seems reasonable are discussed in Sec. 7.3; we simply note here that the same distortion products (nonlinear terms) in the expansion of the autocorrelation function for the output of a nonlinearity with a gaussian input which account for the difference in the forms of the power spectral density functions at input and output also change the form of the distribution function. If the linear part of the system, in returning this nonlinearity output back to its input, fails to filter these higher-frequency distortion products adequately, a dynamic representation of the static nonlinearity would be in order, but *not* one which depends on the assumption of a gaussian input to the nonlinearity.

If one agreed on the use of a static gain to approximate a static nonlinearity, there would still remain several reasonable choices for the criterion under which this gain is to be chosen. One line of approach was initiated by Booton (Refs. 5, 6), who approximated a nonlinearity with a random input by a gain chosen to minimize the mean-squared difference between the outputs of the nonlinearity and its approximator. This concept was extended by Somerville and Atherton (Ref. 42) to a multiple-gain representation of a nonlinearity, with an input having components of several characteristic forms, such as a random process and a sinusoid. Each component of the input is transmitted through a separate gain, and these gains are chosen to minimize the mean-squared error in the total approximation. It has been demonstrated in Sec. 1.5 that minimization of the mean-squared error in the approximation is achieved by the gain which makes the covariance between the component of input that the gain multiplies and the output of the approximating gain equal to the covariance between that component of input and the output of the nonlinearity. Merhav (Ref. 26) suggests the use of covariance equivalence as a more satisfying definition for equivalent linearization, but the results of this definition are identical with those based on minimization of mean-squared approximation error. Another approach is to equate the mean-squared values at the outputs of the nonlinearity and its approximator. Barrett and Coales (Ref. 4) described this procedure, which they attributed to Burt. Later Axelby (Ref. 3) represented a nonlinearity with an input bias signal and random process by two gains chosen to reproduce the mean and mean-squared values of the output of the nonlinearity. Kazakov (Ref. 17) discussed both this method and Booton's at

an early date. A third doctrine, espoused by Sawaragi and Takahashi (Ref. 39), and later by Sridhar and Oldenburger (Ref. 43), requires the calculation of the autocorrelation function of the output of the nonlinearity for the assumed input. This is done in series form in which there appear terms that are linearly related to the input autocorrelation function, higher-order distortion terms, and cross-modulation terms, if more than one input component is present. The approximating gains are selected to reproduce at their outputs the linear terms in the expansion of the nonlinearity output autocorrelation function.

Smith (Refs. 40, 41) attacked the problem of nonlinear feedback systems with random inputs, using the method of functional analysis. With this analytic tool and extensive experimentation, he compared a number of quasi-linear methods for the approximation of nonlinearities. He concluded that if the assumption of a gaussian input to the nonlinearity holds to a good approximation, all these methods give very good results. If one of the methods fails, they all do, since the most important reason for the failure is the failure of the gaussian assumption which is common to all. In these cases for the systems which Smith studied, the method of Booton or its extension by Somerville and Atherton was somewhat to be preferred. Since, in addition, it is preferable on the basis of the computation required, the method of quasi-linearization based on minimization of the mean-squared approximation error, or the method of covariance equivalence, has been pursued in this book.

Having decided upon this criterion, we take satisfaction in noting that the question of a static vs. dynamic quasi-linear approximator need not be considered a separate issue. The most general linear approximator was taken as the starting point in Chap. 1: a parallel set of dynamic linear operators, one to operate on each of the distinguishable components of input. The necessary and sufficient conditions which these operators must satisfy to minimize the mean-squared approximation error were then derived, and those cases in which the optimum transfer is just a static gain appeared as a consequence of the theory. Booton (Ref. 5) had noted the important fact that for an unbiased gaussian input to a static single-valued nonlinearity, the optimum (in the least-mean-squared-error sense) quasi-linear approximator is a static gain. Later Nuttall (Ref. 32) investigated this property more generally.

It should be observed that entirely different avenues of approach can be taken to the study of certain nonlinear systems with random inputs, approaches which do not employ a quasi-linear approximation for the nonlinearity at all. For relay control systems it is possible to write the switching conditions for the relay in terms of the time response of the linear part of the system, and the random input. From this the second-order statistics of the half-periods of the oscillation and of any signal in the system

can be calculated. This is a direct extension of the methods of Tsytkin and others, which were summarized in Sec. 3.8. This procedure, using different analytic formulations, has been discussed by Katkovnik and Pervozvanskii (Ref. 16), Morosanov (Ref. 28), and Tsytkin (Ref. 45). It does not fall within the theme of this book, however, and will not be considered further.

## 7.2 CALCULATION OF RANDOM-INPUT DESCRIBING FUNCTIONS (RIDFs)

We now address our attention to the calculation of random-input describing functions (RIDFs) for specific nonlinearities with rather general inputs. A nonlinear device with an input consisting of the sum of components of several characteristic forms presents a complicated situation. A quasi-linear approximation to the nonlinearity in this case results in a set of approximating gains, each of which is dependent upon all the input components. One might expect the calculation of these gains to be a rather formidable task; in this the reader will not be disappointed. However, the degree to which this theory proves useful to the practicing engineer depends directly upon his facility to calculate, and then to manipulate, the required RIDFs. This section is intended to be of assistance in the former problem.

It was determined in Chap. I that the most general nonlinearity input which need be considered is the sum of a single bias component, a single gaussian component, and an arbitrary number of sinusoids. For the purpose of this section and Appendix E, we shall take the input to be the sum of a bias, a gaussian signal, and a single sinusoid. For those cases in which it is necessary to include more than one sinusoid, the extension of these results is evident, but of course the complexity of the problem increases. In this case, then, the nonlinearity input is

$$x(t) = B + r(t) + A \sin(\omega t + \theta) \quad (7.2-1)$$

$B$ ,  $A$ , and  $\omega$  are deterministic parameters;  $r(0)$  is a random variable having a normal distribution; and  $\theta$  is a random variable having a uniform distribution over an interval of  $2\pi$  radians. The expectations in the definitions of the approximating gains are thus taken over the distributions of  $r(0)$ , which we shall just write as  $r$ , and  $\theta$ . The joint probability density function for these random variables is

$$f_2(r, \theta) = \frac{1}{2\pi} \cdot \frac{1}{\sqrt{2\pi}\sigma} \exp\left(-\frac{r^2}{2\sigma^2}\right) \quad (7.2-2)$$

over the intervals  $-\infty < r < \infty$  and  $0 \leq \theta \leq 2\pi$ . In this expression,  $\sigma$  is the standard deviation of the unbiased stationary gaussian random process  $r(t)$ .

In this section, attention is centered on static single-valued nonlinearities for which the output  $y(t)$  can be written unambiguously as  $y[x(t)]$ . The gain to the bias component of the input is, from Eq. (1.5-27),

$$\begin{aligned} N_B &= \frac{1}{B} \overline{y[x(0)]} \\ &= \frac{1}{(2\pi)^{\frac{1}{2}} \sigma B} \int_0^{2\pi} d\theta \int_{-\infty}^{\infty} dr y(B + r + A \sin \theta) \exp\left(-\frac{r^2}{2\sigma^2}\right) \end{aligned} \quad (7.2-3)$$

The gain to the random component of the input, according to Eq. (1.5-51), is

$$\begin{aligned} N_R &= \frac{1}{\sigma^2} \overline{y[x(0)]r(0)} \\ &= \frac{1}{(2\pi)^{\frac{1}{2}} \sigma^3} \int_0^{2\pi} d\theta \int_{-\infty}^{\infty} dr y(B + r + A \sin \theta) r \exp\left(-\frac{r^2}{2\sigma^2}\right) \end{aligned} \quad (7.2-4)$$

The gain to the sinusoidal component of the input is given by Eq. (1.5-36) to be

$$\begin{aligned} N_A &= \frac{2}{A} \overline{y[x(0)] \sin \theta} \\ &= \frac{2}{(2\pi)^{\frac{1}{2}} \sigma A} \int_0^{2\pi} d\theta \int_{-\infty}^{\infty} dr y(B + r + A \sin \theta) \sin \theta \exp\left(-\frac{r^2}{2\sigma^2}\right) \end{aligned} \quad (7.2-5)$$

We shall first document several useful nonlinearities for which analytic RIDFs can be derived. This is followed by a numerical integration procedure simple enough for use in hand calculation. In addition to this, it is clear that a standard digital-computer program for RIDF calculation, together with certain function subroutines, will be a most valuable asset to one who is to make regular use of RIDF theory. This matter is also discussed.

## POLYNOMIAL NONLINEARITIES

Nonlinear functions of the form

$$y(x) = \sum_n c_n x^n \quad (7.2-6)$$

can be integrated to analytic expressions for the RIDFs. It is possible to do the  $r$  and  $\theta$  integrations in either order, but the algebra is a little simpler if the  $r$  integration is done first. This integration is expedited by writing the nonlinear function in terms of the Hermite polynomials, to take advantage of their orthogonality. As given in Appendix H, the first few of these

polynomials are

$$\begin{aligned} H_0(u) &= 1 \\ H_1(u) &= u \\ H_2(u) &= u^2 - 1 \\ H_3(u) &= u^3 - 3u \end{aligned}$$

and in general,

$$H_{k+1}(u) = uH_k(u) - kH_{k-1}(u)$$

The orthogonality conditions are

$$\frac{1}{\sqrt{2\pi}} \int_{-\infty}^{\infty} H_k(u)H_j(u) \exp\left(-\frac{u^2}{2}\right) du = \begin{cases} k! & j = k \\ 0 & j \neq k \end{cases} \quad (7.2-7)$$

If the integrals involved in the expressions for  $N_B$ ,  $N_R$ , and  $N_A$  are to be put in the form of Eq. (7.2-7), the variable  $r$  must be normalized with respect to the standard deviation  $\sigma$ .

$$v = \frac{r}{\sigma}$$

Thus the first step is to rewrite the original nonlinear function in terms of Hermite polynomials, with  $r$  replaced by  $\sigma v$ .

$$\begin{aligned} y(B + r + A \sin \theta) &= \sum_n c_n(r + B + A \sin \theta)^n \\ &= \sum_n d_n H_n(v) \end{aligned} \quad (7.2-8)$$

where the  $d_n$  will be functions of  $B + A \sin \theta$  and  $\sigma$ . This step can always be taken by starting with the highest power of  $r$  (or  $v$ ) and working toward the lowest.

**Example 7.2-1** Express the cubic nonlinearity in the form of Eq. (7.2-8).

$$y(x) = x^3 \quad (7.2-9)$$

Thus

$$\begin{aligned} y(B + r + A \sin \theta) &= (\sigma v + B + A \sin \theta)^3 \\ &= \sigma^3 v^3 + 3\sigma^2 v^2(B + A \sin \theta) \\ &\quad + 3\sigma v(B + A \sin \theta)^2 + (B + A \sin \theta)^3 \\ &= \sigma^3 H_3(v) + 3(B + A \sin \theta)\sigma^2 H_2(v) \\ &\quad + 3[(B + A \sin \theta)^2 \sigma + \sigma^3] H_1(v) \\ &\quad + [(B + A \sin \theta)^3 + 3(B + A \sin \theta)\sigma^2] H_0(v) \\ &= \sum_{n=0}^3 d_n H_n(v) \end{aligned} \quad (7.2-10)$$



With the nonlinearity expressed in terms of Hermite polynomials, the  $r$  integration—or with the change of variable, the  $v$  integration—is trivial.

$$\begin{aligned} N_B &= \frac{1}{(2\pi)^{\frac{3}{2}}B} \int_0^{2\pi} d\theta \int_{-\infty}^{\infty} dv \left[ \sum_n d_n H_n(v) \right] H_0(v) \exp\left(-\frac{v^2}{2}\right) \\ &= \frac{1}{2\pi B} \int_0^{2\pi} d_0(B + A \sin \theta, \sigma) d\theta \end{aligned} \tag{7.2-11}$$

$$\begin{aligned} N_R &= \frac{1}{(2\pi)^{\frac{3}{2}}\sigma} \int_0^{2\pi} d\theta \int_{-\infty}^{\infty} dv \left[ \sum_n d_n H_n(v) \right] H_1(v) \exp\left(-\frac{v^2}{2}\right) \\ &= \frac{1}{2\pi\sigma} \int_0^{2\pi} d_1(B + A \sin \theta, \sigma) d\theta \end{aligned} \tag{7.2-12}$$

$$\begin{aligned} N_A &= \frac{2}{(2\pi)^{\frac{3}{2}}A} \int_0^{2\pi} d\theta \int_{-\infty}^{\infty} dv \left[ \sum_n d_n H_n(v) \right] H_0(v) \sin \theta \exp\left(-\frac{v^2}{2}\right) \\ &= \frac{1}{\pi A} \int_0^{2\pi} d_0(B + A \sin \theta, \sigma) \sin \theta d\theta \end{aligned} \tag{7.2-13}$$

The remaining  $\theta$  integration is an ordinary harmonic analysis of the functions  $d_0$  and  $d_1$ , which, when expanded, are simply polynomial expressions in  $A \sin \theta$ . The required integrals have already been considered in Chap. 6, and are rewritten here in the form

$$\begin{aligned} \int_0^{2\pi} (\sin \theta)^n d\theta &= 0 && n \text{ odd} \\ &= 2\sqrt{\pi} \frac{\Gamma\left(\frac{n+1}{2}\right)}{\Gamma\left(\frac{n+2}{2}\right)} && n \text{ even and } \geq 0 \tag{7.2-14} \\ &= 2\pi \frac{(1)(3)(5)\cdots(n-1)}{(2)(4)(6)\cdots(n)} && n \text{ even and } \geq 2 \end{aligned}$$

Use of this integral permits the RIDFs to be calculated in closed analytic form.

**Example 7.2-1 (continued)** Complete the calculation of the RIDFs for the cubic nonlinearity. We have

$$\begin{aligned} d_0 &= (B + A \sin \theta)^3 + 3(B + A \sin \theta)\sigma^2 \\ &= A^3 \sin^3 \theta + 3A^2B \sin^2 \theta + 3A(B^2 + \sigma^2) \sin \theta + B^3 + 3B\sigma^2 \end{aligned}$$

$$\begin{aligned} \text{and} \quad d_1 &= 3[(B + A \sin \theta)^2 \sigma + \sigma^3] \\ &= 3\sigma(A^2 \sin^2 \theta + 2AB \sin \theta + B^2 + \sigma^2) \end{aligned}$$

$$\begin{aligned} \text{Thus} \quad N_B &= \frac{1}{2\pi B} \int_0^{2\pi} d_0 d\theta \\ &= \frac{1}{B} \left( \frac{3}{2} A^2 B + B^3 + 3B\sigma^2 \right) \\ &= B^2 + 3\sigma^2 + \frac{3}{2} A^2 \end{aligned} \tag{7.2-15}$$

$$\begin{aligned} N_R &= \frac{1}{2\pi\sigma} \int_0^{2\pi} d_1 d\theta \\ &= \frac{3\sigma}{\sigma} \left( \frac{1}{2} A^2 + B^2 + \sigma^2 \right) \\ &= 3B^2 + 3\sigma^2 + \frac{3}{2} A^2 \end{aligned} \tag{7.2-16}$$

$$\begin{aligned} \text{and} \quad N_A &= \frac{1}{\pi A} \int_0^{2\pi} d_0 \sin \theta d\theta \\ &= \frac{2}{A} \left[ \frac{3}{8} A^3 + \frac{3}{2} A(B^2 + \sigma^2) \right] \\ &= 3B^2 + 3\sigma^2 + \frac{3}{4} A^2 \end{aligned} \tag{7.2-17}$$

It may be noted that the expressions for  $N_B$  and  $N_A$  reduce to the corresponding DIDs of Eqs. (6.2-27) and (6.2-26) in the case of  $\sigma = 0$ .

No other type of nonlinearity yields RIDFs in so simple a form as this.

A modified form of polynomial nonlinearity is often of interest, a function which includes both odd and even powers of  $x$  but which is defined as an odd function.

$$\begin{aligned} y(x) &= \sum_n c_n x^n \quad x \geq 0 \\ y(-x) &= -y(x) \end{aligned} \tag{7.2-18}$$

The terms which are odd powers of  $x$  have the same analytic definition over the full range of  $x$ , and can be integrated by the procedure given above. However, the terms which are even powers of  $x$  have a different analytic definition for  $x < 0$  than for  $x \geq 0$  and require a different treatment. The general term of order  $n$ , with  $n$  even, would be written

$$y(x) = \begin{cases} x^n & x \geq 0 \\ -x^n & x < 0 \end{cases} \tag{7.2-19}$$

The  $r$  integrations in the expressions for  $N_B$  and  $N_A$  are then

$$\begin{aligned} & \frac{1}{\sqrt{2\pi}\sigma} \int_{-\infty}^{\infty} y(B + r + A \sin \theta) \exp\left(-\frac{r^2}{2\sigma^2}\right) dr \\ &= \frac{1}{\sqrt{2\pi}} \int_{-\infty}^{\infty} y(\sigma v + B + A \sin \theta) \exp\left(-\frac{v^2}{2}\right) dv \\ &= \frac{-1}{\sqrt{2\pi}} \int_{-\frac{B+A \sin \theta}{\sigma}}^{-\frac{B+A \sin \theta}{\sigma}} (\sigma v + B + A \sin \theta)^n \exp\left(-\frac{v^2}{2}\right) dv \\ & \quad + \frac{1}{\sqrt{2\pi}} \int_{-\frac{B+A \sin \theta}{\sigma}}^{\infty} (\sigma v + B + A \sin \theta)^n \exp\left(-\frac{v^2}{2}\right) dv \quad (7.2-20) \end{aligned}$$

Expansion of the integrand yields both odd and even powers of  $v$ . The required integrals are then of the form

$$\frac{1}{\sqrt{2\pi}} \int v^n \exp\left(-\frac{v^2}{2}\right) dv = -\frac{1}{\sqrt{2\pi}} \int v^{n-1} d\left[\exp\left(-\frac{v^2}{2}\right)\right] \quad (7.2-21)$$

Repeated integration by parts gives the result

$$\begin{aligned} & \frac{1}{\sqrt{2\pi}} \int v^n \exp\left(-\frac{v^2}{2}\right) dv \\ &= -\frac{1}{\sqrt{2\pi}} \left[ v^{n-1} \exp\left(-\frac{v^2}{2}\right) + (n-1)v^{n-3} \exp\left(-\frac{v^2}{2}\right) \right. \\ & \quad \left. + \cdots + (n-1)(n-3) \cdots (2) \exp\left(-\frac{v^2}{2}\right) \right] \quad n \text{ odd and } \geq 3 \\ &= -\frac{1}{\sqrt{2\pi}} \left[ v^{n-1} \exp\left(-\frac{v^2}{2}\right) + (n-1)v^{n-3} \exp\left(-\frac{v^2}{2}\right) \right. \\ & \quad \left. + \cdots + (n-1)(n-3) \cdots (1)v \exp\left(-\frac{v^2}{2}\right) \right] \\ & \quad + (n-1)(n-3) \cdots (1) \frac{1}{\sqrt{2\pi}} \int \exp\left(-\frac{v^2}{2}\right) dv \quad n \text{ even and } \geq 2 \end{aligned} \quad (7.2-22)$$

This last integration in the expression for even  $n$  cannot be written in closed form. It is tabulated as a function of the upper limit of integration for a lower limit of  $-\infty$ , as in Burington (Ref. 7). We shall be dealing repeatedly with this function, and for convenience shall designate it the *probability integral*.

$$PI(v) = \frac{1}{\sqrt{2\pi}} \int_{-\infty}^v \exp\left(-\frac{u^2}{2}\right) du \quad (7.2-23)$$

The integrand of the probability integral is the normal probability function which also appears throughout this work. We shall refer to it simply as the *probability function*.

$$\text{PF}(v) = \frac{1}{\sqrt{2\pi}} \exp\left(-\frac{v^2}{2}\right) \quad (7.2-24)$$

The integral above is conveniently written in terms of these functions.

$$\begin{aligned} & \frac{1}{\sqrt{2\pi}} \int v^n \exp\left(-\frac{v^2}{2}\right) dv \\ &= -[v^{n-1} + (n-1)v^{n-3} + \cdots + (n-1)(n-3)\cdots(2)]\text{PF}(v) && n \text{ odd and } \geq 3 \\ &= -\text{PF}(v) && n = 1 \\ &= -[v^{n-1} + (n-1)v^{n-3} + \cdots + (n-1)(n-3)\cdots(1)v]\text{PF}(v) \\ &\quad + (n-1)(n-3)\cdots(1)\text{PI}(v) && n \text{ even and } \geq 2 \\ &= \text{PI}(v) && n = 0 \end{aligned} \quad (7.2-25)$$

This integral form suffices for the  $r$  integration in the expressions for  $N_B$  and  $N_A$ , as given in Eq. (7.2-20), and also for the  $r$  integration in the expression for  $N_R$ , which is of similar form. However, the  $\theta$  integration cannot now be done analytically.

This solution is adequate for cases in which there is no sinusoidal component in the nonlinearity input, and thus no  $\theta$  integration in the expressions for  $N_B$  and  $N_R$ . In that case,

$$x(t) = B + r(t) \quad (7.2-26)$$

$$N_B = \frac{1}{\sqrt{2\pi}\sigma B} \int_{-\infty}^{\infty} y(B+r) \exp\left(-\frac{r^2}{2\sigma^2}\right) dr \quad (7.2-27)$$

$$N_R = \frac{1}{\sqrt{2\pi}\sigma^3} \int_{-\infty}^{\infty} y(B+r)r \exp\left(-\frac{r^2}{2\sigma^2}\right) dr \quad (7.2-28)$$

**Example 7.2-2** The ideal-relay characteristic

$$y(x) = \begin{cases} D & x > 0 \\ 0 & x = 0 \\ -D & x < 0 \end{cases} \quad (7.2-29)$$

has in this case the RIDFs

$$\begin{aligned}
 N_B &= \frac{-D}{\sqrt{2\pi B}} \int_{-\infty}^{-B/\sigma} \exp\left(-\frac{v^2}{2}\right) dv + \frac{D}{\sqrt{2\pi B}} \int_{-B/\sigma}^{\infty} \exp\left(-\frac{v^2}{2}\right) dv \\
 &= \frac{D}{B} \left[ -\text{PI}\left(-\frac{B}{\sigma}\right) + 1 - \text{PI}\left(-\frac{B}{\sigma}\right) \right] \\
 &= \frac{D}{B} \left[ 2\text{PI}\left(\frac{B}{\sigma}\right) - 1 \right]
 \end{aligned} \tag{7.2-30}$$

and

$$\begin{aligned}
 N_R &= \frac{-D}{\sqrt{2\pi\sigma}} \int_{-\infty}^{-B/\sigma} v \exp\left(-\frac{v^2}{2}\right) dv + \frac{D}{\sqrt{2\pi\sigma}} \int_{-B/\sigma}^{\infty} v \exp\left(-\frac{v^2}{2}\right) dv \\
 &= \frac{D}{\sigma} \left[ \text{PF}\left(-\frac{B}{\sigma}\right) + \text{PF}\left(-\frac{B}{\sigma}\right) \right] \\
 &= 2 \frac{D}{\sigma} \text{PF}\left(\frac{B}{\sigma}\right)
 \end{aligned} \tag{7.2-31}$$

In the preceding example, certain evident properties of the probability function and probability integral were used:

$$\text{PF}(\infty) = \text{PF}(-\infty) = 0 \tag{7.2-32}$$

$$\text{PI}(\infty) = 1 \tag{7.2-33}$$

$$\text{PI}(-\infty) = 0 \tag{7.2-34}$$

$$\text{PF}(-v) = \text{PF}(v) \tag{7.2-35}$$

$$\text{PI}(-v) = 1 - \text{PI}(v) \tag{7.2-36}$$

If the RIDFs are required for nonlinearities of this modified polynomial form with a sinusoidal input component as well, the  $\theta$  integration requires integrating terms of the form  $\text{PF}[(B + A \sin \theta)/\sigma]$  and  $\text{PI}[(B + A \sin \theta)/\sigma]$ . This must be done numerically. We shall return to the question of numerical integration for RIDFs later in this section.

## HARMONIC NONLINEARITIES

Nonlinear functions of the form

$$y(x) = \sum_n c_n \sin m_n x \tag{7.2-37}$$

permit analytic evaluation of the RIDFs. The representation of the nonlinear function in terms of an integral transform is especially convenient in this instance. This procedure was employed in Chap. 5, both for analytic

arguments and for TSIDF evaluation; we shall employ the same transform here.

$$y(x) = \frac{1}{2\pi} \int_{-\infty}^{\infty} Y(ju) \exp(jux) du \quad (7.2-38)$$

where 
$$Y(ju) = \int_{-\infty}^{\infty} y(x) \exp(-jux) dx \quad (7.2-39)$$

in those cases for which the transform exists. Writing  $y(x)$  in terms of its transform in Eqs. (7.2-3) to (7.2-5) gives, for the case of a bias plus gaussian plus single-sinusoid input,

$$\begin{aligned} N_B &= \frac{1}{(2\pi)^{\frac{1}{2}}\sigma B} \int_0^{2\pi} d\theta \int_{-\infty}^{\infty} dr \int_{-\infty}^{\infty} du Y(ju) \exp\left[-\frac{r^2}{2\sigma^2} + ju(B+r+A\sin\theta)\right] \\ &= \frac{1}{(2\pi)^{\frac{1}{2}}B} \int_{-\infty}^{\infty} du Y(ju) \exp(juB) \int_0^{2\pi} d\theta \exp(juA\sin\theta) \int_{-\infty}^{\infty} dv \\ &\quad \times \exp\left[-\frac{1}{2}(v^2 - 2ju\sigma v)\right] \end{aligned} \quad (7.2-40)$$

Completing the square in the exponent for the  $v$  integral gives

$$\frac{1}{\sqrt{2\pi}} \int_{-\infty}^{\infty} dv \exp\left[-\frac{1}{2}(v^2 - 2ju\sigma v)\right] = \exp\left(-\frac{\sigma^2 u^2}{2}\right) \quad (7.2-41)$$

From the definition of the Bessel function,

$$J_n(x) = \frac{1}{2\pi} \int_0^{2\pi} \exp[j(x\sin\theta - n\theta)] d\theta \quad (7.2-42)$$

the  $\theta$  integral is recognized as  $J_0(Au)$ . Putting these results in Eq. (7.2-40), we have

$$N_B = \frac{1}{2\pi B} \int_{-\infty}^{\infty} Y(ju) J_0(Au) \exp\left(-\frac{\sigma^2 u^2}{2} + juB\right) du \quad (7.2-43)$$

This form of the result is quite convenient. Alternatively, one can complete the square in the exponent to get

$$N_B = \frac{1}{\sqrt{2\pi B}} \text{PF}\left(\frac{B}{\sigma}\right) \int_{-\infty}^{\infty} Y(ju) J_0(Au) \exp\left[-\frac{1}{2}(\sigma u - jB/\sigma)^2\right] du \quad (7.2-44)$$

Using similar manipulations, the gain to the gaussian signal is written

$$\begin{aligned} N_R &= \frac{1}{(2\pi)^{\frac{1}{2}}\sigma^3} \int_0^{2\pi} d\theta \int_{-\infty}^{\infty} dr \int_{-\infty}^{\infty} du Y(ju) r \exp\left[-\frac{r^2}{2\sigma^2} + ju(B+r+A\sin\theta)\right] \\ &= \frac{1}{(2\pi)^{\frac{1}{2}}\sigma} \int_{-\infty}^{\infty} du Y(ju) \exp(juB) \int_0^{2\pi} d\theta \exp(juA\sin\theta) \int_{-\infty}^{\infty} dv v \\ &\quad \times \exp\left[-\frac{1}{2}(v^2 - 2ju\sigma v)\right] \\ &= \frac{j}{2\pi} \int_{-\infty}^{\infty} Y(ju) J_0(Au) u \exp\left(-\frac{\sigma^2 u^2}{2} + juB\right) du \end{aligned} \quad (7.2-45)$$

Alternatively,

$$N_R = \frac{j}{\sqrt{2\pi}} \text{PF}\left(\frac{B}{\sigma}\right) \int_{-\infty}^{\infty} Y(ju) J_0(Au) u \exp\left[-\frac{1}{2}\left(\sigma u - j\frac{B}{\sigma}\right)^2\right] du \quad (7.2-46)$$

Finally,

$$\begin{aligned} N_A &= \frac{2}{(2\pi)^{\frac{1}{2}}\sigma A} \int_0^{2\pi} d\theta \int_{-\infty}^{\infty} dr \int_{-\infty}^{\infty} du Y(ju) \sin \theta \\ &\quad \times \exp\left[-\frac{r^2}{2\sigma^2} + ju(B + r + A \sin \theta)\right] \\ &= \frac{2}{(2\pi)^{\frac{1}{2}}A} \int_{-\infty}^{\infty} du Y(ju) \exp(juB) \int_0^{2\pi} d\theta \sin \theta \exp(juA \sin \theta) \int_{-\infty}^{\infty} dv \\ &\quad \times \exp\left[-\frac{1}{2}(v^2 - 2ju\sigma v)\right] \\ &= \frac{j}{\pi A} \int_{-\infty}^{\infty} Y(ju) J_1(Au) \exp\left(-\frac{\sigma^2 u^2}{2} + jBu\right) du \end{aligned} \quad (7.2-47)$$

or

$$N_A = \sqrt{\frac{2}{\pi}} \frac{j}{A} \text{PF}\left(\frac{B}{\sigma}\right) \int_{-\infty}^{\infty} Y(ju) J_1(Au) \exp\left[-\frac{1}{2}\left(\sigma u - j\frac{B}{\sigma}\right)^2\right] du \quad (7.2-48)$$

In the  $\theta$  integration for  $N_A$ ,  $\sin \theta$  is written in terms of  $\exp(j\theta)$  and  $\exp(-j\theta)$ . Integration then gives a term  $J_{-1}(Au)$  and a term  $J_1(Au)$ , which can be collected, using the property  $J_{-n}(x) = -J_n(x)$  for  $n$  odd.

In the case of each of these gains, the original double-integral expression involving the nonlinear function has been reduced to a single integral involving the transform of the nonlinear function. For some nonlinearities  $Y(ju)$  is easier to integrate than  $y(x)$ .

**Example 7.2-3** Calculate the RIDFs for the harmonic nonlinearity. The general term in the sum of Eq. (7.2-37) is

$$y(x) = \sin mx \quad (7.2-49)$$

The transform of this is

$$\begin{aligned} Y(ju) &= \int_{-\infty}^{\infty} \sin mx \exp(-jux) dx \\ &= \frac{1}{2j} \int_{-\infty}^{\infty} [\exp[j(m-u)x] - \exp[-j(m+u)x]] dx \\ &= \frac{\pi}{j} [\delta(u-m) - \delta(u+m)] \end{aligned} \quad (7.2-50)$$

This function can readily be integrated according to Eqs. (7.2-43), (7.2-45), and (7.2-47) to give analytic expressions for the RIDFs for the general harmonic-term nonlinear function.

$$\begin{aligned}
 N_B &= \frac{1}{2\pi B} \int_{-\infty}^{\infty} \frac{\pi}{j} [\delta(u-m) - \delta(u+m)] J_0(Au) \exp\left(-\frac{\sigma^2 u^2}{2} + jBu\right) du \\
 &= \frac{1}{2Bj} \left[ J_0(Am) \exp\left(-\frac{\sigma^2 m^2}{2} + jBm\right) - J_0(-Am) \exp\left(-\frac{\sigma^2 m^2}{2} - jBm\right) \right] \\
 &= \frac{1}{B} J_0(Am) \exp\left(-\frac{m^2 \sigma^2}{2}\right) \frac{1}{2j} [\exp(jBm) - \exp(-jBm)] \\
 &= \frac{1}{B} \sin mB \exp\left(-\frac{m^2 \sigma^2}{2}\right) J_0(mA) \tag{7.2-51}
 \end{aligned}$$

$$\begin{aligned}
 N_R &= \frac{j}{2\pi} \int_{-\infty}^{\infty} \frac{\pi}{j} [\delta(u-m) - \delta(u+m)] J_0(Au) u \exp\left(-\frac{\sigma^2 u^2}{2} + jBu\right) du \\
 &= \frac{1}{2} \left[ J_0(Am) m \exp\left(-\frac{\sigma^2 m^2}{2} + jBm\right) + J_0(-Am) m \exp\left(-\frac{\sigma^2 m^2}{2} - jBm\right) \right] \\
 &= J_0(Am) m \exp\left(-\frac{m^2 \sigma^2}{2}\right) \frac{1}{2} [\exp(jBm) + \exp(-jBm)] \\
 &= m \cos mB \exp\left(-\frac{m^2 \sigma^2}{2}\right) J_0(mA) \tag{7.2-52}
 \end{aligned}$$

$$\begin{aligned}
 N_A &= \frac{j}{\pi A} \int_{-\infty}^{\infty} \frac{\pi}{j} [\delta(u-m) - \delta(u+m)] J_1(Au) \exp\left(-\frac{\sigma^2 u^2}{2} + jBu\right) du \\
 &= \frac{1}{A} \left[ J_1(Am) \exp\left(-\frac{\sigma^2 m^2}{2} + jBm\right) - J_1(-Am) \exp\left(-\frac{\sigma^2 m^2}{2} - jBm\right) \right] \\
 &= \frac{1}{A} J_1(Am) \exp\left(-\frac{m^2 \sigma^2}{2}\right) [\exp(jBm) + \exp(-jBm)] \\
 &= \frac{2}{A} \cos mB \exp\left(-\frac{m^2 \sigma^2}{2}\right) J_1(mA) \tag{7.2-53}
 \end{aligned}$$

In this development, use is made of the property of Bessel functions that  $J_n(x)$  is an odd function of  $x$  if  $n$  is odd and is an even function of  $x$  if  $n$  is even.

These are the RIDFs for the general term of a harmonic nonlinearity. If a nonlinear function is a linear combination of terms of this type, as in Eq. (7.2-37), the RIDFs are the corresponding linear combinations of the terms given in Eqs. (7.2-51) to (7.2-53).

### PIECEWISE-LINEAR NONLINEARITIES

A great many nonlinearities of common interest are composed of a sequence of straight-line segments. If we allow the possibility of discontinuous jumps between these segments, this family of nonlinearities assumes even greater proportions. It will be of value to treat this family in as general a way as possible.



To this end consider a general linear segment as pictured in Fig. 7.2-1. Any nonlinear function consisting of straight-line segments with or without jumps between them can be decomposed into segments of this form. If the contribution of this general segment to the integrals defining the RIDFs can be calculated, the RIDFs for any piecewise-linear nonlinearity could be synthesized as the sums of such contributions. Unfortunately, it will not be possible to carry out this program analytically in the case of the three-component input. In the double-integral expressions for the RIDFs [Eqs. (7.2-3) to (7.2-5)], either the  $r$  or the  $\theta$  integration can be carried out for the general linear segment, but in each case this gives rise to functions which do not permit the second integration to be done analytically. This suffices for the case where either the sinusoid or the gaussian process is missing from the input, but if both are present, the RIDF calculation must be completed by numerical integration.

The limits of integration for a nonlinear function of finite extent are much simpler to handle if the  $r$  integration is done first. The general linear segment of Fig. 7.2-1 is nonzero over the interval  $x_1 < x < x_2$ . The  $r$  and  $\theta$  integrations must then be carried out over the region in the  $r, \theta$  plane, which satisfies simultaneously the inequalities

$$x_1 < B + r + A \sin \theta < x_2$$

and

$$0 < \theta < 2\pi \tag{7.2-54}$$

This region is pictured in Fig. 7.2-2 for the case  $A < (x_2 - x_1)/2$ . The  $\theta$  integration, if done first, would be over different intervals of  $\theta$  for  $r$  in different regions, and these intervals are different for larger values of  $A$  relative to  $x_2 - x_1$ . On the other hand, if the  $r$  integration is done first, it is always over the interval  $x_1 - B - A \sin \theta < r < x_2 - B - A \sin \theta$ . The subsequent  $\theta$  integration is then simply over the interval  $0 < \theta < 2\pi$ .

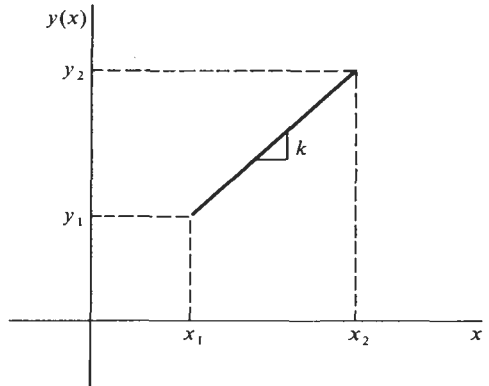


Figure 7.2-1 General segment of a piecewise-linear nonlinearity.

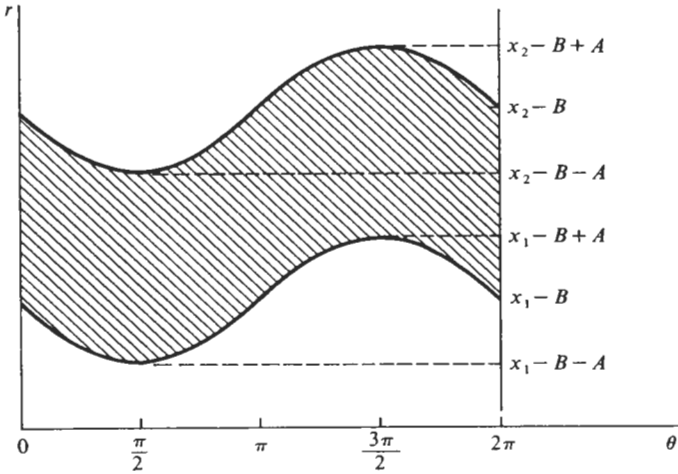


Figure 7.2-2 Region of integration for the general linear segment.

In the expressions for  $N_B$  and  $N_A$  [Eqs. (7.2-3) and (7.2-5)], the  $r$  integration is of the form

$$I_1 = \frac{1}{\sqrt{2\pi}\sigma} \int_{-\infty}^{\infty} y(B + r + A \sin \theta) \exp\left(-\frac{r^2}{2\sigma^2}\right) dr \quad (7.2-55)$$

For the general linear segment of Fig. 7.2-1, this becomes

$$\begin{aligned} I_1 &= \frac{1}{\sqrt{2\pi}} \int_{v_1}^{v_2} [y_1 + k(B + \sigma v + A \sin \theta - x_1)] \exp\left(-\frac{v^2}{2}\right) dv \\ &= [y_1 + k(B + A \sin \theta - x_1)][\text{PI}(v_2) - \text{PI}(v_1)] + k\sigma[\text{PF}(v_1) - \text{PF}(v_2)] \\ &= [y_1 - k\sigma v_1][\text{PI}(v_2) - \text{PI}(v_1)] + k\sigma[\text{PF}(v_1) - \text{PF}(v_2)] \end{aligned} \quad (7.2-56)$$

using the integral form of Eq. (7.2-25).  $v_1$  and  $v_2$  are the end points of the integration, given by

$$v_1 = \frac{1}{\sigma} (x_1 - B - A \sin \theta) \quad (7.2-57)$$

$$v_2 = \frac{1}{\sigma} (x_2 - B - A \sin \theta) \quad (7.2-58)$$

This form of  $I_1$  holds for any linear segment of finite extent, or one which extends to  $x \rightarrow +\infty$ , in which case  $v_2 \rightarrow +\infty$ . To be applicable to a

segment which extends to  $x \rightarrow -\infty$ , Eq. (7.2-56) must be rewritten in terms of  $y_2$ .

$$y_2 = y_1 + k(x_2 - x_1) \quad (7.2-59)$$

$$\begin{aligned} I_1 &= [y_2 - k(x_2 - x_1) + k(B + A \sin \theta - x_1)][\text{PI}(v_2) - \text{PI}(v_1)] \\ &\quad + k\sigma[\text{PF}(v_1) - \text{PF}(v_2)] \\ &= (y_2 - k\sigma v_2)[\text{PI}(v_2) - \text{PI}(v_1)] + k\sigma[\text{PF}(v_1) - \text{PF}(v_2)] \end{aligned} \quad (7.2-60)$$

This also holds for any segment of finite extent, or one which extends to  $x \rightarrow -\infty$ , in which case  $v_1 \rightarrow -\infty$ .

The  $r$  integration in the expression for  $N_R$  [Eq. (7.2-4)] is of the form

$$\begin{aligned} I_2 &= \frac{1}{\sqrt{2\pi\sigma^2}} \int_{-\infty}^{\infty} y(B + r + A \sin \theta)r \exp\left(-\frac{r^2}{2\sigma^2}\right) dr \\ &= \frac{1}{\sqrt{2\pi}} \int_{v_1}^{v_2} [y_1 + k(B + \sigma v + A \sin \theta - x_1)]v \exp\left(-\frac{v^2}{2}\right) dv \\ &= [y_1 - k\sigma v_1][\text{PF}(v_1) - \text{PF}(v_2)] + k\sigma[v_1 \text{PF}(v_1) - v_2 \text{PF}(v_2)] \\ &\quad + k\sigma[\text{PI}(v_2) - \text{PI}(v_1)] \\ &= y_1[\text{PF}(v_1) - \text{PF}(v_2)] + k\sigma[\text{PI}(v_2) - \text{PI}(v_1) - (v_2 - v_1)\text{PF}(v_2)] \end{aligned} \quad (7.2-61)$$

In terms of  $y_2$  this is rewritten

$$I_2 = y_2[\text{PF}(v_1) - \text{PF}(v_2)] + k\sigma[\text{PI}(v_2) - \text{PI}(v_1) - (v_2 - v_1)\text{PF}(v_1)] \quad (7.2-62)$$

When evaluating Eq. (7.2-61) for a segment which extends to plus infinity, it should be noted that

$$\lim_{v_2 \rightarrow \infty} (v_2 - v_1)\text{PF}(v_2) = 0 \quad (7.2-63)$$

$$\text{Similarly,} \quad \lim_{v_1 \rightarrow -\infty} (v_2 - v_1)\text{PF}(v_1) = 0 \quad (7.2-64)$$

These integrals,  $I_1$  and  $I_2$ , are functions of the parameters which characterize the linear segment, and of  $\sigma$ ,  $B$ , and  $A \sin \theta$ . Indicating in the notation only the dependence on  $A \sin \theta$ , the RIDFs for the segment are now written as

$$N_B = \frac{1}{2\pi B} \int_0^{2\pi} I_1(A \sin \theta) d\theta \quad (7.2-65)$$

$$N_R = \frac{1}{2\pi\sigma} \int_0^{2\pi} I_2(A \sin \theta) d\theta \quad (7.2-66)$$

$$N_A = \frac{1}{\pi A} \int_0^{2\pi} I_1(A \sin \theta) \sin \theta d\theta \quad (7.2-67)$$

which are simply in the form of a harmonic analysis of the functions  $I_1$  and  $I_2$ . As in the case of modified polynomial nonlinearities, the integrals of  $\text{PF}(x)$  and  $\text{PI}(x)$  are required. For a piecewise-linear nonlinearity which consists of the sum of a number of these segments, the individual contributions to the RIDFs can be calculated according to Eqs. (7.2-65) to (7.2-67) and then added, or more efficiently, the individual  $I_1$  and  $I_2$  contributions can be added first and then integrated at once with respect to  $\theta$ .

If the nonlinearity input is taken to include only a bias and a gaussian signal, the integrals  $I_1$  and  $I_2$  constitute a complete solution for the RIDFs. In that case

$$x(t) = B + r(t) \quad (7.2-68)$$

$$\begin{aligned} N_B &= \frac{1}{\sqrt{2\pi\sigma B}} \int_{-\infty}^{\infty} y(B+r) \exp\left(-\frac{r^2}{2\sigma^2}\right) dr \\ &= \frac{1}{B} I_1(A=0) \end{aligned} \quad (7.2-69)$$

$$\begin{aligned} N_R &= \frac{1}{\sqrt{2\pi\sigma^3}} \int_{-\infty}^{\infty} y(B+r)r \exp\left(-\frac{r^2}{2\sigma^2}\right) dr \\ &= \frac{1}{\sigma} I_2(A=0) \end{aligned} \quad (7.2-70)$$

These contributions to the RIDFs corresponding to each linear segment can very easily be added to give a closed-form expression for the approximating gains for any piecewise-linear nonlinearity.

**Example 7.2-4** Calculate the RIDFs for the relay with dead-zone nonlinearity (see Fig. 7.2-3) for the case of a bias plus gaussian input ( $A=0$ ).

$$\text{Segment 1:} \quad \begin{cases} x_1 = -\infty & v_1 = -\infty \\ x_2 = -\delta & v_2 = \frac{-\delta - B}{\sigma} \\ y_2 = -D & k = 0 \end{cases}$$

From Eqs. (7.2-60) and (7.2-62) it follows that

$$\begin{aligned} I_1(A=0) &= -D \left[ \text{PI}\left(\frac{-\delta - B}{\sigma}\right) - \text{PI}(-\infty) \right] \\ &= -D \left[ 1 - \text{PI}\left(\frac{\delta + B}{\sigma}\right) \right] \end{aligned}$$

$$\begin{aligned} \text{and} \quad I_2(A=0) &= -D \left[ \text{PF}(-\infty) - \text{PF}\left(\frac{-\delta - B}{\sigma}\right) \right] \\ &= D \text{PF}\left(\frac{\delta + B}{\sigma}\right) \end{aligned}$$

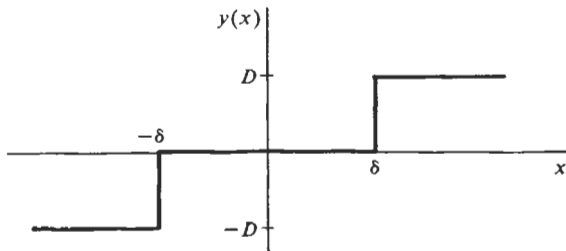


Figure 7.2-3 Nonlinear characteristic for Example 7.2-4.

Segment 2:

$$\begin{cases} x_1 = \delta & v_1 = \frac{\delta - B}{\sigma} \\ x_2 = \infty & v_2 = \infty \\ y_1 = D & k = 0 \end{cases}$$

Similarly, Eqs. (7.2-56) and (7.2-61) yield

$$\begin{aligned} I_1(A = 0) &= D \left[ \text{PI}(\infty) - \text{PI}\left(\frac{\delta - B}{\sigma}\right) \right] \\ &= D \left[ 1 - \text{PI}\left(\frac{\delta - B}{\sigma}\right) \right] \end{aligned}$$

and

$$\begin{aligned} I_2(A = 0) &= D \left[ \text{PF}\left(\frac{\delta - B}{\sigma}\right) - \text{PF}(\infty) \right] \\ &= D \text{PF}\left(\frac{\delta - B}{\sigma}\right) \end{aligned}$$

Finally, Eqs. (7.2-69) and (7.2-70) give

$$N_B = \frac{D}{B} \left[ \text{PI}\left(\frac{\delta + B}{\sigma}\right) - \text{PI}\left(\frac{\delta - B}{\sigma}\right) \right] \tag{7.2-71}$$

$$N_R = \frac{D}{\sigma} \left[ \text{PF}\left(\frac{\delta + B}{\sigma}\right) + \text{PF}\left(\frac{\delta - B}{\sigma}\right) \right] \tag{7.2-72}$$

These expressions reduce to the RIDFs for the ideal relay [Eqs. (7.2-30) and (7.2-31)] in the case  $\delta = 0$ .

### NUMERICAL INTEGRATION FOR HAND CALCULATION

The majority of nonlinear functions do not permit an analytic integration of the expressions defining the RIDFs. The user must then be prepared to calculate RIDFs through numerical, graphical, or other means of integration. One evident procedure for approximate RIDF calculation is to approximate

the given nonlinear function by one for which the RIDFs can more easily be calculated. Either a polynomial or harmonic-function approximation to the nonlinearity will lead to analytic expressions for approximate RIDFs using the results derived above. A straight-line-segment approximation permits one integration to be done analytically.

However, the approximation of one function by others is in itself a substantial task; so we look to other means of RIDF calculation which use the given nonlinear function directly. The most convenient technique for general use is *numerical*. We present, first, an approximate procedure simple enough for hand calculation, and then consider the problem of more exact numerical integration by machine calculation.

The double-integral expressions for the RIDFs in the case of a three-component input [Eqs. (7.2-3) to (7.2-5)] can be integrated in either order. If the  $r$  integration is done first, these expressions might be written

$$N_B = \frac{1}{B} \frac{1}{2\pi} \int_0^{2\pi} \left[ \frac{1}{\sqrt{2\pi}\sigma} \int_{-\infty}^{\infty} y(B + r + A \sin \theta) \exp\left(-\frac{r^2}{2\sigma^2}\right) dr \right] d\theta \quad (7.2-73)$$

$$N_R = \frac{1}{\sigma} \frac{1}{2\pi} \int_0^{2\pi} \left[ \frac{1}{\sqrt{2\pi}\sigma^2} \int_{-\infty}^{\infty} y(B + r + A \sin \theta) r \exp\left(-\frac{r^2}{2\sigma^2}\right) dr \right] d\theta \quad (7.2-74)$$

$$N_A = \frac{1}{A} \frac{1}{\pi} \int_0^{2\pi} \left[ \frac{1}{\sqrt{2\pi}\sigma} \int_{-\infty}^{\infty} y(B + r + A \sin \theta) \exp\left(-\frac{r^2}{2\sigma^2}\right) dr \right] \sin \theta d\theta \quad (7.2-75)$$

If the  $\theta$  integration were done first, these expressions would be written

$$N_B = \frac{1}{B} \frac{1}{\sqrt{2\pi}\sigma} \int_{-\infty}^{\infty} \left[ \frac{1}{2\pi} \int_0^{2\pi} y(B + r + A \sin \theta) d\theta \right] \exp\left(-\frac{r^2}{2\sigma^2}\right) dr \quad (7.2-76)$$

$$N_R = \frac{1}{\sigma} \frac{1}{\sqrt{2\pi}\sigma^2} \int_{-\infty}^{\infty} \left[ \frac{1}{2\pi} \int_0^{2\pi} y(B + r + A \sin \theta) d\theta \right] r \exp\left(-\frac{r^2}{2\sigma^2}\right) dr \quad (7.2-77)$$

$$N_A = \frac{1}{A} \frac{1}{\sqrt{2\pi}\sigma} \int_{-\infty}^{\infty} \left[ \frac{1}{\pi} \int_0^{2\pi} y(B + r + A \sin \theta) \sin \theta d\theta \right] \exp\left(-\frac{r^2}{2\sigma^2}\right) dr \quad (7.2-78)$$

In either case there appear just four types of integrals:

$$I_1(c) = \frac{1}{\sqrt{2\pi\sigma}} \int_{-\infty}^{\infty} y(c+r) \exp\left(-\frac{r^2}{2\sigma^2}\right) dr \quad (7.2-79)$$

$$I_2(c) = \frac{1}{\sqrt{2\pi\sigma^2}} \int_{-\infty}^{\infty} y(c+r)r \exp\left(-\frac{r^2}{2\sigma^2}\right) dr \quad (7.2-80)$$

$$I_3(c) = \frac{1}{2\pi} \int_0^{2\pi} y(c+A \sin \theta) d\theta \quad (7.2-81)$$

$$I_4(c) = \frac{1}{\pi} \int_0^{2\pi} y(c+A \sin \theta) \sin \theta d\theta \quad (7.2-82)$$

In an  $r$  integration,  $c = B + A \sin \theta$ , and in a  $\theta$  integration,  $c = B + r$ ; but in either case,  $c$  is just a constant during that integration. The present functions  $I_1$  and  $I_2$  are consistent with those used before in the case of the general segment of a piecewise-linear nonlinearity.

Any one of these RIDFs is now calculated by first evaluating the inner integral for a number of values of  $c$ . The resulting function of  $c$  is plotted to permit interpolating for other values of  $c$  as required in the evaluation of the outer integral. In the calculation of the second integral, this function of  $c$  resulting from the first integration plays the role of a new nonlinear function. Each of these expressions can be interpreted in terms of a "modified nonlinearity" if one desires to do so. For example, in the calculation of  $N_B$  and  $N_R$ , using Eqs. (7.2-76) and (7.2-77), the inner integral is of the form  $I_3(c)$ . This function may be considered a modified nonlinearity in which the effect of the sinusoid on the gains of the original nonlinearity to the bias and the gaussian signal has been accounted for. The outer integrals which involve  $I_3(B+r)$  in the integrand are exactly the expressions for  $N_B$  and  $N_R$  for the nonlinear function  $I_3(x)$ , having an input  $x(t) = B + r(t)$ . Similarly, in the calculation of  $N_B$  and  $N_A$ , using Eqs. (7.2-73) and (7.2-75), the outer integrals are exactly the expressions for  $N_B$  and  $N_A$  for the nonlinear function  $I_1(x)$  with the input  $x(t) = B + A \sin(\omega t + \theta)$ , where  $I_1(c)$  resulting from the inner integral may be interpreted as a modified nonlinearity, which accounts for the effect of the random process on the gains of the original nonlinearity to the bias and sinusoid. This modified-nonlinearity concept, which has been referred to by many writers [Somerville and Atherton (Ref. 42) were probably first among them] extends also to cases of additional sinusoids at the input.

We now develop an approximate integration procedure for each of the

required integral forms. For the first [Eq. (7.2-79)] we write

$$\begin{aligned}
 I_1(c) &= \frac{1}{\sqrt{2\pi}\sigma} \int_{-\infty}^{\infty} y(c+r) \exp\left(-\frac{r^2}{2\sigma^2}\right) dr \\
 &= \int_{-\infty}^{\infty} y(c+\sigma v) \frac{1}{\sqrt{2\pi}} \exp\left(-\frac{v^2}{2}\right) dv \\
 &= \int_0^1 y(c+\sigma v) d[\text{PI}(v)] \\
 &\approx \delta[\text{PI}(v)] \sum_i y(c+\sigma v_i)
 \end{aligned} \tag{7.2-83}$$

where the integral is approximated by a finite sum, and equal increments of  $\text{PI}(v)$  are assumed. The  $v_i$  are the values of  $v$  at which the nonlinear function is evaluated. There are a number of reasonable ways to choose the values of  $v_i$  to use. One would be to take the mid-range value of  $v$  corresponding to each incremental range of  $\text{PI}(v)$ . Probably better than this, on the average, would be the values of  $v_i$  which give the correct answer for some average form of  $y(x)$ , say, a linear function in each interval. This is the same approach taken in Chap. 2 for the approximate numerical calculation of the DF. This choice of the  $v_i$  results in the trapezoidal integration rule, approximating the integral of the actual  $y(x)$  by the integral of a function which is equal to  $y(x)$  at each end of the integration step and linear between these points. The exact integral over a linear segment of  $y(x)$  is given in Eq. (7.2-56). The corresponding contribution to the sum of Eq. (7.2-83) can be equated to this to determine the appropriate value of  $v_i$ . The result of this calculation is

$$v_i = \frac{\text{PF}(v_1) - \text{PF}(v_2)}{\text{PI}(v_2) - \text{PI}(v_1)} \tag{7.2-84}$$

The interpretation of this expression is as follows: A value for  $\delta[\text{PI}(v)]$  is chosen to give the desired number of intervals. Ten intervals, for example, correspond to  $\delta[\text{PI}(v)] = 0.1$ . The first interval corresponds to  $\text{PI}(v)$  ranging from 0 to 0.1; the second to  $\text{PI}(v)$  ranging from 0.1 to 0.2; etc. For each of these intervals,  $v_1$  is the value of  $v$  corresponding to  $\text{PI}(v)$  at the lower end of the interval, and  $v_2$  is the value of  $v$  corresponding to  $\text{PI}(v)$  at the upper end of the interval.  $v_i$  is then the value of  $v$ , intermediate to  $v_1$  and  $v_2$ , at which  $y(c+\sigma v_i)$  should be evaluated to yield the correct integral over this interval if  $y(x)$  were linear over the interval.  $\text{PI}(v)$  ranges monotonically from 0 to 1; so  $\delta[\text{PI}(v)] = 1/n$ , where  $n$  is the number of intervals to be used. Equation (7.2-83) is then written

$$I_1(c) \approx \frac{1}{n} \sum_{i=1}^n y(c+\sigma v_i) \tag{7.2-85}$$

The values of  $v_i$  for  $n = 10$  and  $20$  are given in Table 7.2-1.



The second integral [Eq. (7.2-80)] is written

$$\begin{aligned}
 I_2(c) &= \frac{1}{\sqrt{2\pi\sigma^2}} \int_{-\infty}^{\infty} y(c+r)r \exp\left(-\frac{r^2}{2\sigma^2}\right) dr \\
 &= \int_{-\infty}^{\infty} y(c+\sigma v) \frac{1}{\sqrt{2\pi}} v \exp\left(-\frac{v^2}{2}\right) dv \\
 &= \int_{-\infty < v < \infty} y(c+\sigma v) d[-PF(v)] \\
 &\approx |\delta[PF(v)]| \sum_i S_i y(c+\sigma v_i) \\
 &\approx \frac{1}{n} \sqrt{\frac{2}{\pi}} \sum_{i=1}^n S_i y(c+\sigma v_i) \quad n \text{ even} \quad (7.2-86)
 \end{aligned}$$

In this case the additional factor  $S_i$  is required to indicate the sign of  $\delta[-PF(v)]$  in each interval; thus  $S_i = -1$  for  $v_i < 0$  and  $+1$  for  $v_i > 0$ .  $PF(v)$  ranges from 0 to  $1/\sqrt{2\pi}$  in the first  $n/2$  steps and then back to 0 in the next  $n/2$ . The values of  $v_i$  which yield the correct integral over an interval for which  $y(x)$  is linear are given by

$$v_i = \frac{v_2 PF(v_2) - v_1 PF(v_1) - PI(v_2) + PI(v_1)}{PF(v_2) - PF(v_1)} \quad (7.2-87)$$

$v_1$  and  $v_2$  refer in this case to the left- and right-hand values of  $v$  at the ends of each interval of  $PF(v)$ . The  $v_i$  for  $n = 10$  and  $20$  are tabulated in Table 7.2-1.

The third integral [Eq. (7.2-81)] is treated in a similar way. Note that

$$\begin{aligned}
 I_3(c) &= \frac{1}{2\pi} \int_0^{2\pi} y(c+A \sin \theta) d\theta \\
 &= \frac{1}{\pi} \int_{-\pi/2}^{\pi/2} y(c+A \sin \theta) d\theta \quad (7.2-88)
 \end{aligned}$$

for any static single-valued nonlinearity, which is a restriction that has been observed throughout this section. Thus

$$\begin{aligned}
 I_3(c) &\approx \frac{\delta\theta}{\pi} \sum_i y(c+A \sin \theta_i) \\
 &\approx \frac{1}{n} \sum_{i=1}^n y(c+A \sin \theta_i) \quad (7.2-89)
 \end{aligned}$$

The appropriate values of  $\sin \theta_i$  for trapezoidal integration accuracy are

$$\sin \theta_i = \frac{\cos \theta_1 - \cos \theta_2}{\theta_2 - \theta_1} \quad (7.2-90)$$

TABLE 7.2-1 ARGUMENT VALUES FOR TRAPEZOIDAL INTEGRATION OF

$I_1$ integration		$I_2$ integration			
$n = 10$	$n = 20$	$n = 10$		$n = 20$	
$v_i$	$v_i$	$S_i$	$v_i$	$S_i$	$v_i$
	-2.0627			-1	-2.5455
	-1.4472			-1	-1.9551
	-1.1532			-1	-1.6677
	-0.9361			-1	-1.4502
	-0.7563			-1	-1.2643
-1.7550	-0.5983	-1	-2.2503	-1	-1.0937
-1.0446	-0.4541	-1	-1.5590	-1	-0.9280
-0.6773	-0.3189	-1	-1.1790	-1	-0.7578
-0.3865	-0.1892	-1	-0.8429	-1	-0.5680
-0.1260	-0.0627	-1	-0.4354	-1	-0.3028
0.1260	0.0627	+1	0.4354	+1	0.3028
0.3865	0.1892	+1	0.8429	+1	0.5680
0.6773	0.3189	+1	1.1790	+1	0.7578
1.0446	0.4541	+1	1.5590	+1	0.9280
1.7550	0.5983	+1	2.2503	+1	1.0937
	0.7563			+1	1.2643
	0.9361			+1	1.4502
	1.1532			+1	1.6677
	1.4472			+1	1.9551
	2.0627			+1	2.5455

where  $\theta_1$  and  $\theta_2$  are the left- and right-hand values of  $\theta$  at the ends of each interval of  $\theta$ . The values of  $\sin \theta_i$  for  $n = 10$  and 20 are tabulated in Table 7.2-1.

The fourth integral [Eq. (7.2-82)] is written

$$\begin{aligned}
 I_4(c) &= \frac{1}{\pi} \int_0^{2\pi} y(c + A \sin \theta) \sin \theta \, d\theta \\
 &= \frac{2}{\pi} \int_{-\pi/2}^{\pi/2} y(c + A \sin \theta) \sin \theta \, d\theta \\
 &= \frac{2}{\pi} \int_{-\pi/2 < \theta < \pi/2} y(c + A \sin \theta) d(-\cos \theta) \\
 &\approx \frac{2}{\pi} |\delta \cos \theta| \sum_i S_i y(c + A \sin \theta_i) \\
 &\approx \frac{1}{n} \frac{4}{\pi} \sum_{i=1}^n S_i y(c + A \sin \theta_i) \quad n \text{ even} \quad (7.2-91)
 \end{aligned}$$

$S_i$  in this case carries the sign of  $-\delta \cos \theta$ , and thus is  $-1$  for  $\sin \theta_i < 0$  and  $+1$  for  $\sin \theta_i > 0$ .  $\cos \theta$  ranges from 0 to 1 in the first  $n/2$  steps and back

## CERTAIN RIDF EXPRESSIONS

$I_3$ integration		$I_4$ integration			
$n = 10$	$n = 20$	$n = 10$		$n = 20$	
$\sin \theta_i$	$\sin \theta_i$	$S_i$	$\sin \theta_i$	$S_i$	$\sin \theta_i$
	-0.9959			-1	-0.9983
	-0.9714			-1	-0.9882
	-0.9229			-1	-0.9678
	-0.8518			-1	-0.9362
	-0.7596			-1	-0.8924
-0.9836	-0.6488	-1	-0.9933	-1	-0.8344
-0.8874	-0.5220	-1	-0.9520	-1	-0.7590
-0.7042	-0.3823	-1	-0.8634	-1	-0.6600
-0.4521	-0.2332	-1	-0.7095	-1	-0.5239
-0.1558	-0.0784	-1	-0.4088	-1	-0.2936
0.1558	0.0784	+1	0.4088	+1	0.2936
0.4521	0.2332	+1	0.7095	+1	0.5239
0.7042	0.3823	+1	0.8634	+1	0.6600
0.8874	0.5220	+1	0.9520	+1	0.7590
0.9836	0.6488	+1	0.9933	+1	0.8344
	0.7596			+1	0.8924
	0.8518			+1	0.9362
	0.9229			+1	0.9678
	0.9714			+1	0.9882
	0.9959			+1	0.9983

to 0 in the next  $n/2$ . The values of  $\sin \theta_i$  for trapezoidal integration accuracy are

$$\sin \theta_i = \frac{\frac{1}{2}(\sin 2\theta_2 - \sin 2\theta_1) - \theta_2 + \theta_1}{2(\cos \theta_2 - \cos \theta_1)} \quad (7.2-92)$$

$\theta_1$  and  $\theta_2$  are the left- and right-hand values of  $\theta$  at the ends of each interval of  $\cos \theta$ . The  $\sin \theta_i$  are tabulated in Table 7.2-1 for  $n = 10$  and 20.

It might be noted that if  $y(x)$  were odd, and  $c = 0$ , which would be true in the case of a single input component—either a gaussian or a sinusoid— $I_1$  and  $I_3$  would be either zero or irrelevant, and  $I_2$  and  $I_4$  could be calculated by integrating over half the range and multiplying the result by 2. In any case, these numerical integrations can be performed quite rapidly by hand. The form of these approximate integrals is especially convenient in that the values of  $y(x)$  which are calculated or read from a graph need not be multiplied by any constants; they are simply added to or subtracted from the total. Having a graph of  $y(x)$  and an adding machine, one can read the required values and add them very quickly.

The accuracy of these approximate integration rules has been checked in the case of the cubic nonlinearity,  $y(x) = x^3$ , which is somewhat typical of smooth nonlinearities, and in the case of the relay with dead zone shown in

TABLE 7.2-2 ACCURACY OF THE TRAPEZOIDAL INTEGRATION RULES

	Cubic nonlinearity		Relay nonlinearity	
	Max error	Av error	Max error	Av error
Integral 1:				
$n = 10$	4.0%	2.5%	7.0%	2.2%
$n = 20$	1.6	1.0	4.5	1.3
Integral 2:				
$n = 10$	6.8	3.4	6.8	1.5
$n = 20$	3.1	1.5	3.9	1.2
Integral 3:				
$n = 10$	0.8	0.4	3.5	0.9
$n = 20$	0.2	0.1	3.9	0.7
Integral 4:				
$n = 10$	1.1	0.4	4.3	0.9
$n = 20$	0.3	0.1	3.6	0.6

*Note:* For the cubic nonlinearity, the errors are given in percent of the true value. For the relay nonlinearity, some of the true values are zero. The errors are thus given in percent of the maximum value of the integral over the 25 values calculated. These maximum values are

$$I_{1,\max} = 1.000$$

$$I_{2,\max} = 0.781$$

$$I_{3,\max} = 1.000$$

$$I_{4,\max} = 1.246$$

Fig. 7.2-3, which is somewhat characteristic of nonlinearities with a discontinuous jump. Each of the four integrals was evaluated at 25 combinations of values for its two parameters. These parameters  $c$ ,  $\sigma$ , and  $A$  (or  $c/\delta$ ,  $\sigma/\delta$ ,  $A/\delta$ , in the case of the relay with dead zone) were taken in all combinations of the values 0.2, 0.5, 1, 2, and 5. The average error over the 25 points and the maximum error is given in Table 7.2-2 for each of these nonlinearities and for  $n = 10$  and 20. For these cases, the 10-point integration rule yields better than 7 percent accuracy, and the 20-point rule, better than 5 percent.

### RIDF CALCULATION BY DIGITAL COMPUTATION

The RIDFs may be calculated as accurately as desired by digital computation using standard numerical integration techniques. This subject needs no discussion here. We simply note that the double integrations required to evaluate the RIDFs for a three-component input can be done much faster if one of the integrations can be done analytically. This was found to be possible for all piecewise-linear nonlinearities and for the modified polynomial nonlinearities, which include even-power terms but are defined to be

odd functions. This represents a very significant family of nonlinear functions. In each case, if the  $r$  integration is done first, the integrand for the  $\theta$  integration includes terms in  $\text{PF}(c + A \sin \theta)$  and  $\text{PI}(c + A \sin \theta)$ . If one has subroutines available in his library to calculate these functions, the integration can be performed very simply. Since  $\text{PF}(x)$  is just an exponential function, a standard exponential subroutine which is available in most computing centers is sufficient. For completeness, however, we suggest an expression which can be used for this purpose.  $\text{PI}(x)$  is less generally available, and we develop an expression for this function which is convenient for machine computation. These functions are pictured in Fig. 7.2-4 for the positive range of  $x$ ; they are defined over the negative range by the fact that  $\text{PF}(x)$  is even and the relation given in Eq. (7.2-36):

$$\text{PI}(-x) = 1 - \text{PI}(x)$$

An approximation for  $\text{PF}(x)$  which is very easy to program and reasonably efficient for machine calculation is derived from the power-series expansion of the function about the origin. This expansion suggests the form

$$\begin{aligned} f_{\text{F}}(x) &= \frac{1/\sqrt{2\pi}}{1 + a_1x^2 + a_2x^4 + \dots + a_nx^{2n}} \\ &= \frac{0.39894229}{1 + \{a_1 + [a_2 + \dots + (a_{n-1} + a_nx^2)x^2 \dots]x^2\}x^2} \end{aligned} \quad (7.2-93)$$

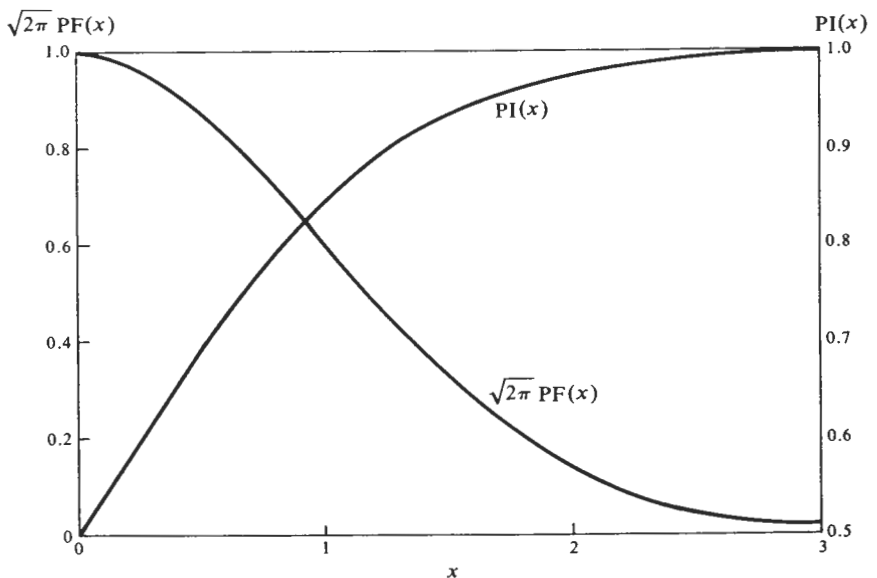


Figure 7.2-4 Normal probability functions.

Using the second, or nested, form, the denominator of this function can be programmed in Fortran by a single DO statement. If this function is to be used primarily for the computation of RIDFs, six-digit accuracy in the approximation is surely adequate, since no more than four-digit accuracy would be of any value in the results of the computation. For  $f_F(x)$ , as given in Eq. (7.2-93), to approximate PF(x) with a maximum error of  $1 \cdot 10^{-6}$  over the full range of  $x$ , requires 14 terms in the denominator. This accuracy is not achieved using values of the  $a_i$  appropriate to the series expansion of PF(x) about the origin, but with  $a_i$  values chosen to minimize the sum of squared errors in the approximation at many points over the range of  $x$ . With the coefficients optimized in this way, the maximum approximation error decreases by a factor of about 2, with each additional term in the expansion. A set of 13 coefficients which yield  $1 \cdot 10^{-6}$  accuracy is given in Table 7.2-3. Note that this approximating function is valid for positive and negative values of  $x$ .

The function PI(x) is surprisingly difficult to approximate well with simple functional forms. For computational efficiency it was found wise to use different approximating functions over two different intervals of  $x$ . The following functional forms are suggested:

$$\begin{aligned}
 f_I(x)_1 &= 0.5 + b_1x + b_2x^3 + b_3x^5 + \cdots + b_nx^{2n-1} \\
 &= 0.5 + \{b_1 + [b_2 + \cdots + (b_{n-1} + b_nx^2)x^2 \cdots]x^2\}x \quad |x| \leq x_M \\
 f_I(x)_2 &= 1 - \frac{1}{c_1x + c_2x^3 + c_3x^5 + \cdots + c_nx^{2n-1}} \\
 &= 1 - \frac{1}{\{c_1 + [c_2 + \cdots + (c_{n-1} + c_nx^2)x^2 \cdots]x^2\}x} \quad x > x_M
 \end{aligned} \tag{7.2-94}$$

The first of these functions is suggested by the form of the power-series expansion of PI(x) about the origin. The second is motivated by the fact that, for large values of  $x$ ,

$$1 - \text{PI}(x) \sim \frac{1}{x} \text{PF}(x) \tag{7.2-95}$$

where this asymptotic equality implies that the ratio of the two members tends to unity as  $x$  tends toward infinity. Even with the range of the function broken into two parts, and with the coefficients  $b_i$  and  $c_i$  optimized on the basis of minimum sum of squared errors, 20 coefficients are required in each of these functions to achieve an error no greater than  $1 \cdot 10^{-6}$  over the full range of  $x$ . The appropriate point at which to break the range of  $x$  is in this case  $x_M = 3.3$ . Sets of coefficients which yield  $1 \cdot 10^{-6}$  accuracy are listed in Table 7.2-3. Note that the first of these functions, for  $x$  of smaller magnitude, is valid for both positive and negative values of  $x$ . The second

**TABLE 7.2-3 COEFFICIENTS IN THE APPROXIMATIONS FOR PF(x) AND PI(x)**

$PF(x) \approx f_F(x) = \frac{0.39894229}{1 + \{a_1 + [a_2 + \cdots + (a_{12} + a_{13}x^2)x^2 \cdots ]x^2\}x^2}$	
$a_1 = 0.50000000$	$a_8 = 0.96881187 \cdot 10^{-7}$
$a_2 = 0.12500000$	$a_9 = 0.53822881 \cdot 10^{-8}$
$a_3 = 0.20833333 \cdot 10^{-1}$	$a_{10} = 0.26911439 \cdot 10^{-9}$
$a_4 = 0.26041665 \cdot 10^{-2}$	$a_{11} = 0.12232172 \cdot 10^{-10}$
$a_5 = 0.26041664 \cdot 10^{-3}$	$a_{12} = 0.50847426 \cdot 10^{-12}$
$a_6 = 0.21701386 \cdot 10^{-4}$	$a_{13} = 0.37188551 \cdot 10^{-13}$
$a_7 = 0.15500990 \cdot 10^{-5}$	
$PI(x) \approx f_I(x)_1 = 0.5 + \{b_1 + [b_2 + \cdots + (b_{19} + b_{20}x^2)x^2 \cdots ]x^2\}x \quad  x  \leq 3.3$	
$b_1 = 0.39894229$	$b_{11} = 0.51124335 \cdot 10^{-11}$
$b_2 = -0.66490381 \cdot 10^{-1}$	$b_{12} = -0.21217608 \cdot 10^{-12}$
$b_3 = 0.99735570 \cdot 10^{-2}$	$b_{13} = 0.81334163 \cdot 10^{-14}$
$b_4 = -0.11873282 \cdot 10^{-2}$	$b_{14} = -0.28965156 \cdot 10^{-15}$
$b_5 = 0.11543468 \cdot 10^{-3}$	$b_{15} = 0.96312710 \cdot 10^{-17}$
$b_6 = -0.94446554 \cdot 10^{-5}$	$b_{16} = -0.30032944 \cdot 10^{-18}$
$b_7 = 0.66596923 \cdot 10^{-6}$	$b_{17} = 0.88214403 \cdot 10^{-20}$
$b_8 = -0.41226666 \cdot 10^{-7}$	$b_{18} = -0.19304226 \cdot 10^{-21}$
$b_9 = 0.22735293 \cdot 10^{-8}$	$b_{19} = 0.18588157 \cdot 10^{-26}$
$b_{10} = -0.11301169 \cdot 10^{-9}$	$b_{20} = 0.24283477 \cdot 10^{-25}$
$PI(x) \approx f_I(x)_2 = 1 - \frac{1}{\{c_1 + [c_2 + \cdots + (c_{19} + c_{20}x^2)x^2 \cdots ]x^2\}x} \quad x > 3.3$	
$c_1 = 0.15145329 \cdot 10^2$	$c_{11} = 0.66769241 \cdot 10^{-9}$
$c_2 = 0.21862164 \cdot 10^1$	$c_{12} = 0.30408705 \cdot 10^{-10}$
$c_3 = 0.37773824$	$c_{13} = 0.13631897 \cdot 10^{-11}$
$c_4 = 0.56444044 \cdot 10^{-1}$	$c_{14} = 0.73926276 \cdot 10^{-13}$
$c_5 = 0.67908929 \cdot 10^{-2}$	$c_{15} = 0.59690240 \cdot 10^{-14}$
$c_6 = 0.66819702 \cdot 10^{-3}$	$c_{16} = 0.56745842 \cdot 10^{-15}$
$c_7 = 0.55222069 \cdot 10^{-4}$	$c_{17} = 0.33853563 \cdot 10^{-16}$
$c_8 = 0.39226156 \cdot 10^{-5}$	$c_{18} = -0.37560769 \cdot 10^{-17}$
$c_9 = 0.24387498 \cdot 10^{-6}$	$c_{19} = 0.32913919 \cdot 10^{-21}$
$c_{10} = 0.13458967 \cdot 10^{-7}$	$c_{20} = 0.18022685 \cdot 10^{-20}$

function, for  $x$  of larger magnitude, is valid only for positive  $x$ ; Eq. (7.2-36) is then used to define the function for negative values.

The integral expression for the describing function gain to each input component is singular for a zero magnitude of that component. Thus one may expect the expression to be poorly behaved numerically for small magnitudes of input. An accurate reference point for small signals is provided by the limiting forms of the describing functions derived in Sec. 1.5. For static single-valued nonlinearities, Eq. (1.5-63) states

$$\lim_{B \rightarrow 0} N_B = N_R(B = 0)$$

and Eq. (1.5-66) gives

$$\lim_{A \rightarrow 0} N_A = N_R(A = 0)$$

The expression for  $N_R$  remains well behaved for small values of  $A$  and  $B$ . No similar expression is known for  $N_R$ , but differentiation of Eq. (1.5-59) with respect to  $B$  reveals the fact that

$$N_R = \frac{d}{dB} (BN_B) \quad (7.2-96)$$

This relation is true in general; in particular, it remains well-behaved for small values of  $\sigma$ .

Another approach to approximate RIDF calculation has been suggested by Atherton (Ref. 2). Using the transform of the nonlinear function, he calculates the RIDFs for a general quantizer nonlinearity in which the steps in both input and output variables are arbitrary. This leads to expressions for the gains in the form of sums of terms which involve the confluent hypergeometric function and the gamma function, among others. These results define the RIDFs for a stepwise approximation to any nonlinearity, and if the required functions are prepared as subroutines for digital computation, the approximation can be made as good as desired.

Having developed adequate means of calculating RIDFs, we now apply them to study the behavior of nonlinear feedback systems with random and other inputs. For convenient reference the three-input RIDFs for several common nonlinearities are presented in Appendix E.

## 7.3 FEEDBACK SYSTEMS WITH RANDOM SIGNALS AND NOISE



function, for  $x$  of larger magnitude, is valid only for positive  $x$ ; Eq. (7.2-36) is then used to define the function for negative values.

The integral expression for the describing function gain to each input component is singular for a zero magnitude of that component. Thus one may expect the expression to be poorly behaved numerically for small magnitudes of input. An accurate reference point for small signals is provided by the limiting forms of the describing functions derived in Sec. 1.5. For static single-valued nonlinearities, Eq. (1.5-63) states

$$\lim_{B \rightarrow 0} N_B = N_R(B = 0)$$

and Eq. (1.5-66) gives

$$\lim_{A \rightarrow 0} N_A = N_R(A = 0)$$

The expression for  $N_R$  remains well behaved for small values of  $A$  and  $B$ . No similar expression is known for  $N_R$ , but differentiation of Eq. (1.5-59) with respect to  $B$  reveals the fact that

$$N_R = \frac{d}{dB} (BN_B) \quad (7.2-96)$$

This relation is true in general; in particular, it remains well-behaved for small values of  $\sigma$ .

Another approach to approximate RIDF calculation has been suggested by Atherton (Ref. 2). Using the transform of the nonlinear function, he calculates the RIDFs for a general quantizer nonlinearity in which the steps in both input and output variables are arbitrary. This leads to expressions for the gains in the form of sums of terms which involve the confluent hypergeometric function and the gamma function, among others. These results define the RIDFs for a stepwise approximation to any nonlinearity, and if the required functions are prepared as subroutines for digital computation, the approximation can be made as good as desired.

Having developed adequate means of calculating RIDFs, we now apply them to study the behavior of nonlinear feedback systems with random and other inputs. For convenient reference the three-input RIDFs for several common nonlinearities are presented in Appendix E.

## 7.3 FEEDBACK SYSTEMS WITH RANDOM SIGNALS AND NOISE

describing functions and by the required satisfaction of a number of simultaneous nonlinear algebraic relations which define the solution. With the thought that it may be prudent to approach these details gradually, this section is restricted to the class of problems in which there is only a single identifiable signal form at the input to the nonlinearity—a gaussian random process. This very important class of problems includes cases in which the system responds to input signals and noise if both are characterized by gaussian processes. We shall even be able to design the Wiener-optimum compensation for such systems, but let us begin with the basic problem of a nonlinear system responding to a single gaussian input.

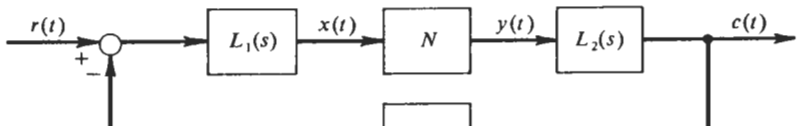
### THE BASIC PROBLEM

The system configuration is shown in Fig. 7.3-1. The system input  $r(t)$  is a stationary gaussian process whose autocorrelation function  $\varphi_{rr}(\tau)$ , or equivalently, whose power spectral density function  $\Phi_{rr}(\omega)$ , is given. If the nonlinearity input  $x(t)$  is to be modeled adequately as a gaussian process, we must assume that the system is not limit cycling. This is a situation precisely paralleling the study of the frequency response of a nonlinear system using the single-sinusoid-input DF as in Chap. 3, and the same observations made earlier regarding the possibility of a system which does not limit-cycle in the absence of input exhibiting one in the presence of an input, or the no-input limit cycle of a system being quenched by an input, are applicable here. With the assumption of no limit cycle,  $x(t)$  is just the random response due to the input, and this response is considered gaussian for the purpose of calculating the describing function for the nonlinearity.

The single-random-input describing function is given by Eq. (7.2-4) with  $A$  and  $B$  equal to zero.

$$\begin{aligned} N_R &= \frac{1}{\sqrt{2\pi\sigma^3}} \int_{-\infty}^{\infty} ry(r) \exp\left(-\frac{r^2}{2\sigma^2}\right) dr \\ &= \frac{1}{\sqrt{2\pi\sigma}} \int_{-\infty}^{\infty} vy(\sigma v) \exp\left(-\frac{v^2}{2}\right) dv \end{aligned} \quad (7.3-1)$$

This integral can be expressed analytically for a number of nonlinearities, in addition to those for which the double-integral expressions of the preceding



section can be evaluated. Some of these expressions are tabulated in Appendix E.

With the effect of the nonlinearity on the input random process expressed in terms of its RIDF, the system has a quasi-linear description. Standard linear theory can then be used to evaluate the mean-squared value of the signal that appears at any point in the loop. In particular, the standard deviation  $\sigma$  of  $x(t)$  is defined by the square root of

$$\sigma^2 = \frac{1}{2\pi} \int_{-\infty}^{\infty} \Phi_{xx}(\omega) d\omega \quad (7.3-2)$$

where 
$$\Phi_{xx}(\omega) = \Phi_{rr}(\omega)H(j\omega)H(-j\omega) \quad (7.3-3)$$

and 
$$H(j\omega) = \frac{L_1(j\omega)}{1 + N_R L_1(j\omega)L_2(j\omega)L_3(j\omega)} \quad (7.3-4)$$

The power spectral density function  $\Phi(\omega)$  was introduced as a function of the real frequency  $\omega$  because only in this case does the function have a clear physical significance: it is the power per unit frequency interval of the harmonic components of the function in the vicinity of  $\omega$ . However, control engineers are more accustomed to functions expressed in terms of the Laplace transform variable  $s$ . Equations (7.3-2) to (7.3-4) can be written in terms of this variable by simply introducing the change of variable  $s = j\omega$ .

$$\sigma^2 = \frac{1}{2\pi j} \int_{-j\infty}^{j\infty} \Phi_{xx}(s) ds \quad (7.3-5)$$

$$\Phi_{xx}(s) = \Phi_{rr}(s)H(s)H(-s) \quad (7.3-6)$$

$$H(s) = \frac{L_1(s)}{1 + N_R L_1(s)L_2(s)L_3(s)} \quad (7.3-7)$$

Strictly speaking, the symbol  $\Phi(s)$  is improper since it does not refer to  $\Phi(\omega)$  with  $\omega$  replaced by  $s$ ; rather,  $\omega$  is replaced by  $s/j$ . However, the symbol is convenient; it is in common use; and no confusion should arise. For rational spectra,  $\omega$  appears only in even powers; so  $\Phi(s)$  is derived from  $\Phi(\omega)$  simply by replacing  $\omega^2$  by  $-s^2$ .

The integral expression for  $\sigma^2$  [Eq. (7.3-5)] can be evaluated analytically if  $\Phi_{xx}(s)$  is a rational function of  $s^2$ . This will be true of any case in which the spectrum  $\Phi_{rr}(s)$  is rational in  $s^2$  and the transfer function  $H(s)$  is rational in  $s$ . For this case, the integral has been evaluated by a number of writers and appears tabulated in many books and journal articles. Table 7.3-1 lists the results for low-ordered spectra; more comprehensive tables may be found in

TABLE 7.3-1 TABULATED INTEGRALS FOR RATIONAL SPECTRA

---


$$V_n = \frac{1}{2\pi j} \int_{-j\infty}^{j\infty} \frac{C(s)C(-s)}{D(s)D(-s)} ds$$

$$C(s) = c_0 + c_1s + c_2s^2 + \cdots + c_{n-1}s^{n-1}$$

$$D(s) = d_0 + d_1s + d_2s^2 + \cdots + d_ns^n$$


---


$$V_1 = \frac{c_0^2}{2d_0d_1}$$

$$V_2 = \frac{c_1^2d_0 + c_0^2d_2}{2d_0d_1d_2}$$

$$V_3 = \frac{c_2^2d_0d_1 + (c_1^2 - 2c_0c_2)d_0d_3 + c_0^2d_2d_3}{2d_0d_3(d_1d_2 - d_0d_3)}$$

$$V_4 = \frac{c_3^2(d_0d_1d_2 - d_0^2d_3) + (c_2^2 - 2c_1c_3)d_0d_1d_4 + (c_1^2 - 2c_0c_2)d_0d_3d_4 + c_0^2(d_2d_3d_4 - d_1d_4^2)}{2d_0d_1(d_1d_2d_3 - d_0d_3^2 - d_1^2d_4)}$$

$$V_5 = \frac{1}{2\Delta} [c_4^2m_0 + (c_3^2 - 2c_2c_4)m_1 + (c_2^2 - 2c_1c_3 + 2c_0c_4)m_2 + (c_1^2 - 2c_0c_2)m_3 + c_0^2m_4]$$

$$m_0 = \frac{1}{d_5} (d_3m_1 - d_1m_2) \quad m_3 = \frac{1}{d_0} (d_2m_2 - d_4m_1)$$

$$m_1 = d_1d_2 - d_0d_3 \quad m_4 = \frac{1}{d_0} (d_2m_3 - d_4m_2)$$

$$m_2 = d_1d_4 - d_0d_5 \quad \Delta = d_0(d_1m_4 - d_3m_3 + d_5m_2)$$


---

simultaneous solution defines the rms value of  $x(t)$  for the given input. The most convenient way to effect the solution is to choose a value of  $\sigma$ , the rms value of  $x(t)$ , and determine the corresponding value of  $N_R$  from Eq. (7.3-1). Equation (7.3-5) is then integrated using this value of  $N_R$ . The mean-squared value of  $r(t)$  can be kept in literal form since it just appears as a multiplying factor for the integral. It is then a simple matter to solve for the rms value of  $r(t)$ , which results in the value of  $\sigma$  originally chosen. This process is repeated with other values of  $\sigma$  until the relation between rms input and rms value of  $x(t)$  is well enough defined to permit interpolation among the results to find the response to a given input.

The solution of  $\sigma_r$  for a given  $\sigma_x$  will always be single-valued. However, different values of  $\sigma_x$  may lead to the same value of  $\sigma_r$ ; that is, for a given input, a *multiple-valued response* may be indicated. Here again is a situation which parallels the sinusoidal response characteristics of similar systems. In that case, a multiple-valued response was termed jump resonance. In this case such a response characteristic is usually called *dual-mode operation*,

error mode tends to be maintained consistently, depending on initial conditions. In the random input case, as one would expect, the system changes apparently at random between the large and small error modes of operation.

Having the value of  $\sigma_x$ , and thus of  $N_R$ , determined for any input, the response at any other point in the loop, such as at the output  $c(t)$ , can be determined by linear methods. The limitation on this is that there must be adequate filtering of the higher-frequency nongaussian content in the output of the nonlinearity. The quasi-linear description of the nonlinearity used here does not model accurately the power spectrum, the distribution, or the mean-squared value of the process at the output of the nonlinearity. The more linear filtering this process experiences, however, the more nearly these characteristics will approach those predicted by this analysis. This too is entirely equivalent to the sinusoidal response situation.

**Example 7.3-1** As an illustration of the procedure just described, consider the second-order system shown in Fig. 7.3-2. The input is a gaussian process, having the power density spectrum

$$\Phi_{rr}(s) = \frac{k}{a^2 - s^2}$$

Using  $V_1$  of Table 7.3-1, the mean-squared value of this input is found to be

$$\sigma_r^2 = \frac{k}{2a}$$

Thus the spectrum can be rewritten to display the mean-squared input directly.

$$\Phi_{rr}(s) = \frac{2a\sigma_r^2}{a^2 - s^2} \quad (7.3-8)$$

The transfer from input to  $x(t)$  is

$$H_x(s) = \frac{X(s)}{R(s)} = \frac{s^2}{s^2 + N_R s + N_R}$$

in which the RIDF is used to characterize the gain of the nonlinearity to its random input.

$$\Phi_{xx}(s) = \frac{2a\sigma_r^2}{a^2 - s^2} H_x(s)H_x(-s)$$

Taking out the factor  $2a\sigma_r^2$ , the function  $C(s)/D(s)$  in the integral form of Table 7.3-1 is identified as

$$\frac{C(s)}{D(s)} = \frac{1}{a + s} \frac{s^2}{s^2 + N_R s + N_R} = \frac{s^2}{s^3 + (a + N_R)s^2 + (1 + a)N_R s + aN_R}$$

$V_3$  from this table then gives

$$\sigma_x^2 = \frac{2a\sigma_r^2 a(1 + a)N_R^2}{s^3 + (a + N_R)s^2 + (1 + a)N_R s + aN_R} = \frac{a\sigma_r^2}{s^3 + (a + N_R)s^2 + (1 + a)N_R s + aN_R} \quad (7.3-9)$$

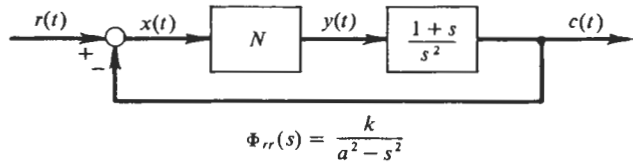


Figure 7.3-2 System of Example 7.3-1.

Equation (7.2-16) with  $A = B = 0$  gives the RIDF as

$$N_R = 3\sigma_x^2 \quad (7.3-10)$$

Now for any given bandwidth of the input spectrum, say,  $a = 1 \text{ sec}^{-1}$ , Eqs. (7.3-9) and (7.3-10) can be solved. For example, take  $\sigma_x = 1$  unit. Then

$$\begin{aligned} N_R &= 3 \\ \sigma_r &= 1\sqrt{3 + \frac{1}{2}} = 1.87 \text{ units} \end{aligned}$$

This calculation is repeated to define a curve of  $\sigma_x$  versus  $\sigma_r$  for a given  $a$ . Then the spectrum of the output is

$$\begin{aligned} \Phi_{cc}(s) &= \frac{2a\sigma_r^2}{a^2 - s^2} H_c(s)H_c(-s) \\ H_c(s) &= \frac{C(s)}{R(s)} = \frac{N_R(s+1)}{s^2 + N_R s + N_R} \end{aligned}$$

and the mean-squared output is

$$\sigma_c^2 = \frac{\sigma_r^2 N_R + a/(1+a)}{N_R N_R + a^2/(1+a)}$$

An example of the response of this nonlinear system to a gaussian input is shown in Fig. 7.3-3, together with the response of the corresponding quasi-linearized system to the same input. The evident close correlation between the outputs,  $c(t)$ , of the two systems indicates the success of the quasi-linear description of the operation of the nonlinearity. Notice that the signal  $y(t)$  is not well modeled. This effect is even more striking if the nonlinearity is an ideal relay, as shown in Fig. 7.3-4.

## ACCURACY

As part of a more comprehensive study, Smith (Refs. 40, 41) checked the accuracy of this analysis, using the system of Fig. 7.3-2 and three different nonlinearities. For each nonlinearity he computed the theoretical relation between  $\sigma_r$  and  $\sigma_x$  for a range of input rms values and for three different bandwidths of the input spectrum. He then measured the actual response of the system as simulated with an analog computer. His results are shown in Figs. 7.3-5 to 7.3-7. The agreement between predicted and observed

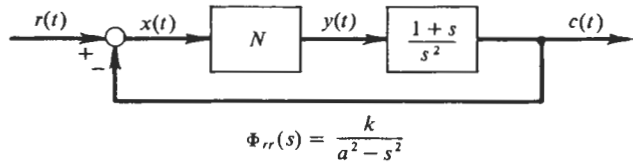


Figure 7.3-2 System of Example 7.3-1.

Equation (7.2-16) with  $A = B = 0$  gives the RIDF as

$$N_R = 3\sigma_x^2 \quad (7.3-10)$$

Now for any given bandwidth of the input spectrum, say,  $a = 1 \text{ sec}^{-1}$ , Eqs. (7.3-9) and (7.3-10) can be solved. For example, take  $\sigma_x = 1$  unit. Then

$$\begin{aligned} N_R &= 3 \\ \sigma_r &= 1\sqrt{3 + \frac{1}{2}} = 1.87 \text{ units} \end{aligned}$$

This calculation is repeated to define a curve of  $\sigma_x$  versus  $\sigma_r$  for a given  $a$ . Then the spectrum of the output is

$$\begin{aligned} \Phi_{cc}(s) &= \frac{2a\sigma_r^2}{a^2 - s^2} H_c(s)H_c(-s) \\ H_c(s) &= \frac{C(s)}{R(s)} = \frac{N_R(s+1)}{s^2 + N_R s + N_R} \end{aligned}$$

and the mean-squared output is

$$\sigma_c^2 = \frac{\sigma_r^2 N_R + a/(1+a)}{N_R N_R + a^2/(1+a)}$$

An example of the response of this nonlinear system to a gaussian input is shown in Fig. 7.3-3, together with the response of the corresponding quasi-linearized system to the same input. The evident close correlation between the outputs,  $c(t)$ , of the two systems indicates the success of the quasi-linear description of the operation of the nonlinearity. Notice that the signal  $y(t)$  is not well modeled. This effect is even more striking if the nonlinearity is an ideal relay, as shown in Fig. 7.3-4.

## ACCURACY

As part of a more comprehensive study, Smith (Refs. 40, 41) checked the accuracy of this analysis, using the system of Fig. 7.3-2 and three different nonlinearities. For each nonlinearity he computed the theoretical relation between  $\sigma_r$  and  $\sigma_x$  for a range of input rms values and for three different bandwidths of the input spectrum. He then measured the actual response of the system as simulated with an analog computer. His results are shown in Figs. 7.3-5 to 7.3-7. The agreement between predicted and observed

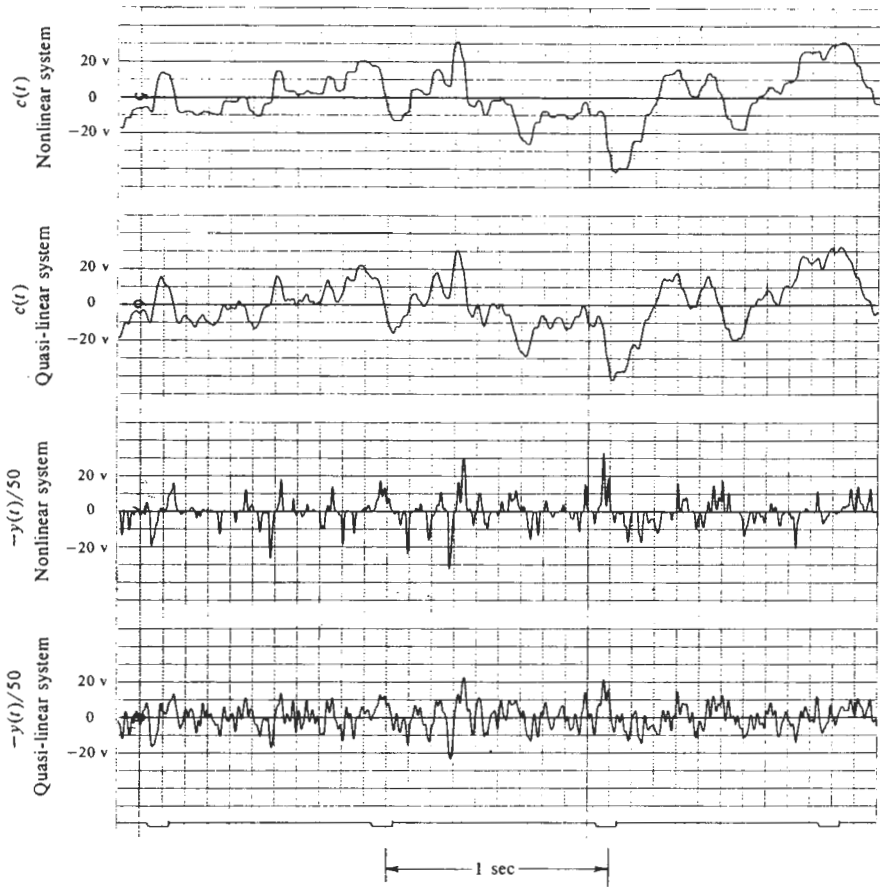


Figure 7.3-3 Sample of response to a random input. Fig. 7.3-2 system, cubic nonlinearity.

decrease can be observed from these results. Note, first, that in every instance in which the data lie close to the line  $\sigma_x = \sigma_r$ , the accuracy is excellent. This is the condition in which the rms error is nearly as large as the rms input, which implies that the feedback in the system is not effective. This occurs mostly for the wideband input. If the fed-back signal is small compared with the input signal,  $x(t)$  has nearly the properties of  $r(t)$ , including its normal distribution. This is the condition under which the analysis was developed. Only when  $\sigma_x$  is appreciably smaller than  $\sigma_r$  does the accuracy decrease, and then not in every case. Note that for the limiter system (Fig. 7.3-7), with  $a = 1$  and small rms input,  $\sigma_x$  is much smaller than



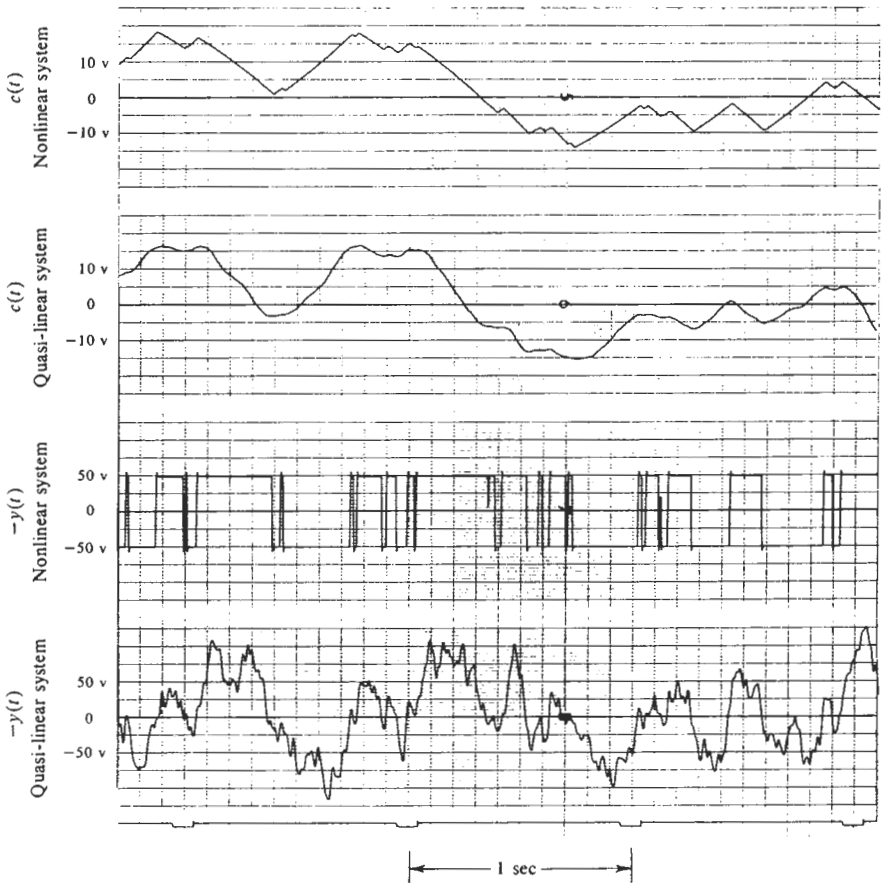


Figure 7.3-4 Sample of response to a random input. System of Fig. 7.3-2, ideal-relay nonlinearity.

An interpretation of these results can be based on the distribution of the signal at the input to the nonlinearity. With a gaussian input to the system,  $x(t)$  can have a distribution which differs significantly from the normal only if an appreciable amount of the distortion generated by the nonlinearity is fed back around the loop to the input to the nonlinearity. An appreciable amount of fed-back signal is implied if the rms error is much smaller than the rms input; this is indeed the intent of the feedback configuration. But in the case of the limiter system with rms error small relative to the value of  $x$  at which limiting occurs, the limiter is only rarely driven into the non-

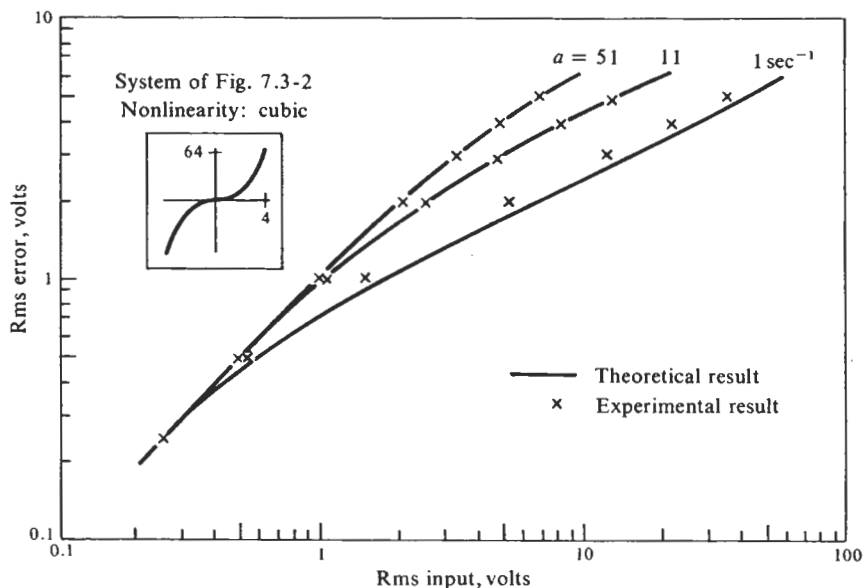
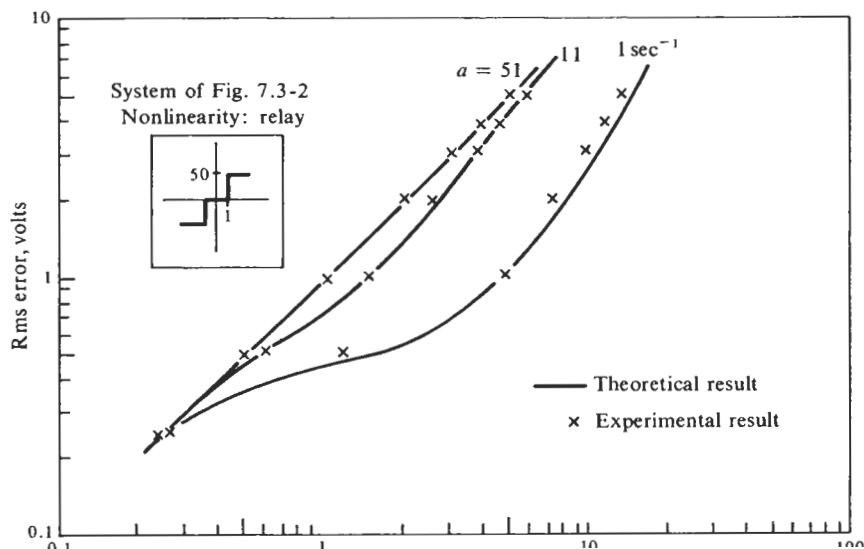


Figure 7.3-5 Response to gaussian input. (Adapted from Smith, Ref. 40.)



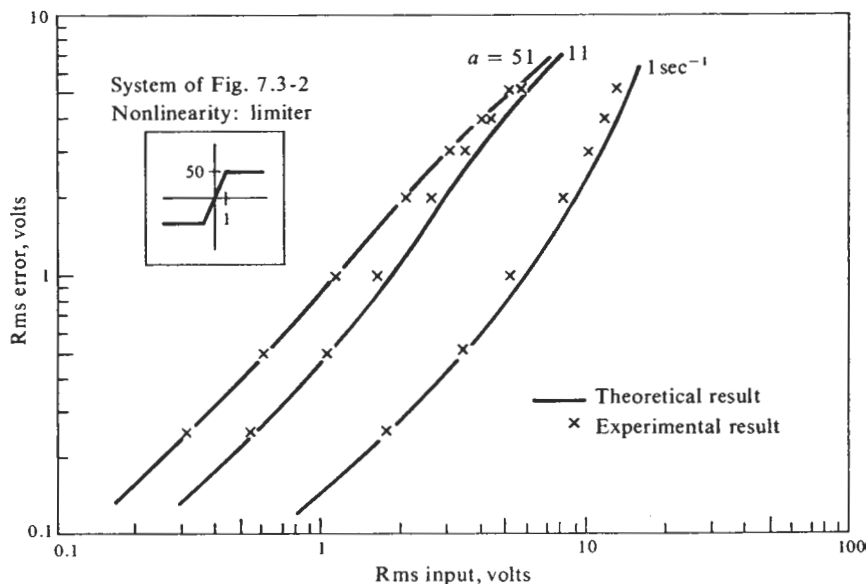


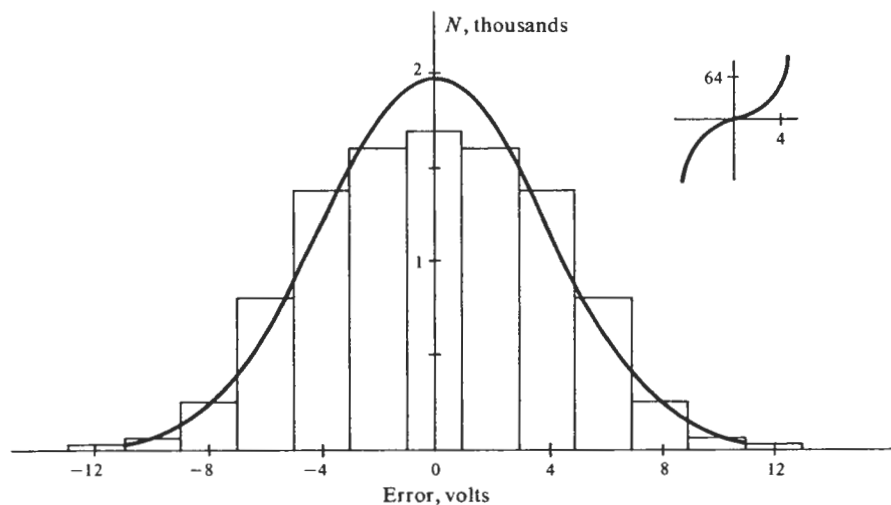
Figure 7.3-7 Response to gaussian input. (Adapted from Smith, Ref. 40.)

must be appreciable compared with the input signal, and it must contain significant nonlinear distortion.

As an indication of the sensitivity of the accuracy of this analysis to the distribution of  $x(t)$ , histograms showing the distribution of the nonlinearity input for three points in Figs. 7.3-5 to 7.3-7, where the theoretical values are most in error, are given in Figs. 7.3-8 to 7.3-10. The normal distribution having the same rms value is shown in each case for reference. These distributions differ quite significantly from the normal, yet the rms error was predicted with less than 10 percent error in each of these cases.

Nikiforuk (Ref. 30) and Nikiforuk and West (Ref. 31) used narrowband filtering to measure the power density spectrum of the output of second-order systems with hard-spring and limiter nonlinearities. Comparison of the output spectrum with the input permits evaluation of the magnitude of the system transfer function over the important frequency range. This experimentally determined frequency response function was compared with that predicted by this analysis and found to agree with better than 20 percent accuracy, except in a low-frequency region, where they questioned their experimental results.

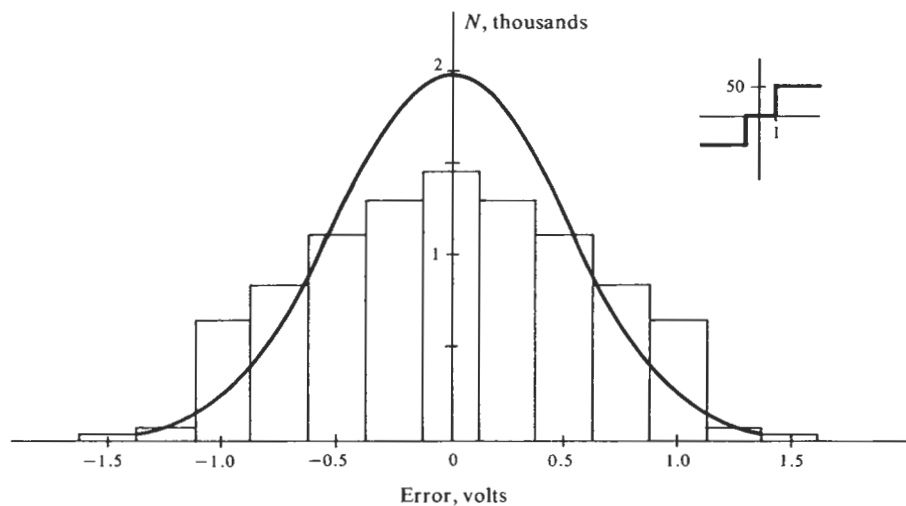
It might be said in summary that the accuracy of the RIDF in dealing with a single random input is of the same order as the accuracy of the ordinary DF



System of Fig. 7.3-2  
 Nonlinearity: cubic

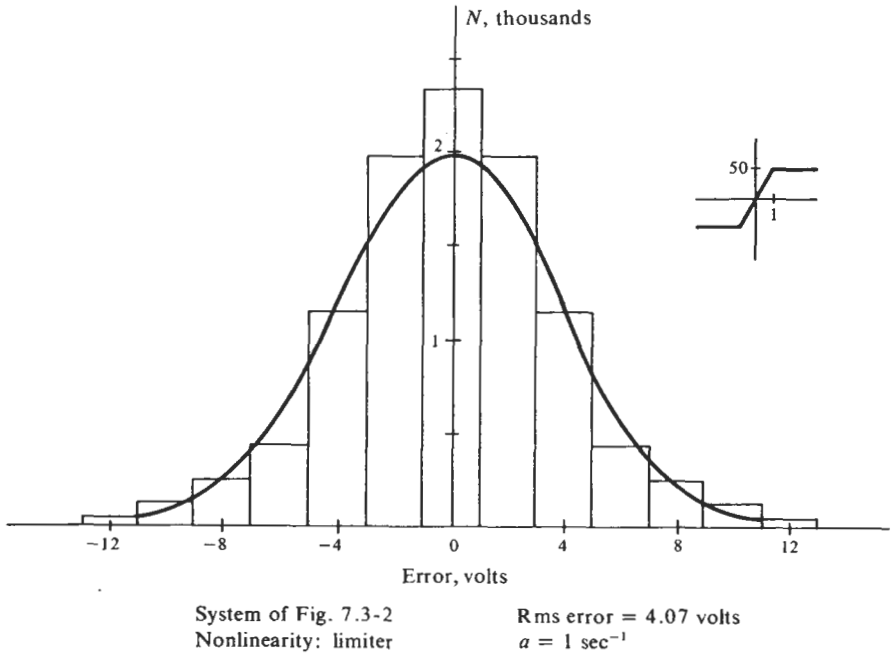
Rms error = 4.0 volts  
 $a = 1 \text{ sec}^{-1}$

Figure 7.3-8 Distribution of 10,000 error samples. (Adapted from Smith, Ref. 40.)



System of Fig. 7.3-2

Rms error = 0.5 volt



**Figure 7.3-10** Distribution of 10,000 error samples. (Adapted from Smith, Ref. 40.)

plants would provide better filtering of nonlinear distortion and permit even better analytic description. When accuracy is degraded, it is due to inadequate filtering of the nongaussian nonlinearity output, which then violates the assumption of a normal distribution at the input to the nonlinearity. Any theory which is to be more accurate than this over a broad range of problems will have to deal with the possibility of a distorted distribution for the nonlinearity input. This, unfortunately, poses a problem which is likely to remain intractable for practical purposes.

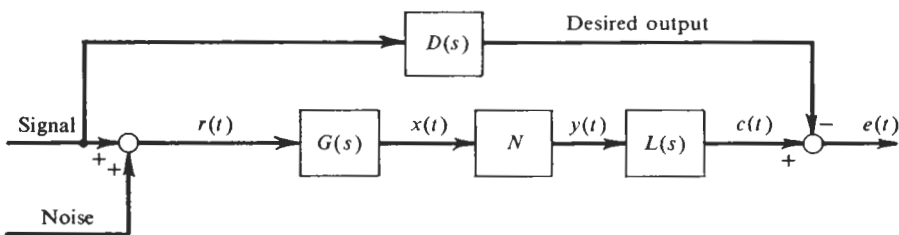
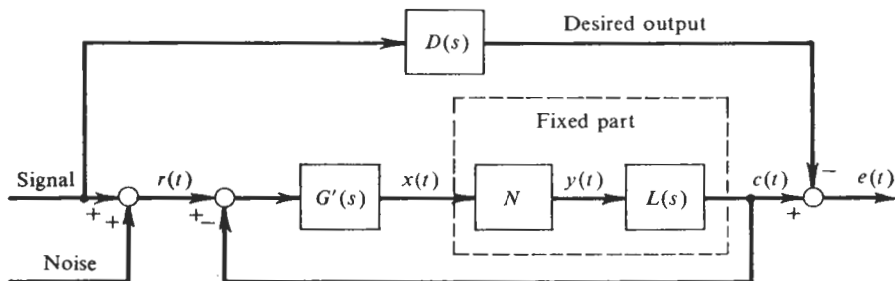
### OPTIMUM LINEAR COMPENSATION

This section has thus far considered the *analysis* of a nonlinear system subjected to a random input. We turn now to the problem of the *synthesis*, or design, of such systems under stated sets of conditions. One of the classics among optimal design problems is the Wiener problem of the separation of a signal from noise with a linear filter. The extension of the solution to the Wiener problem to the design of optimum linear compensation for a system

The conditions of the problem are these:

1. The system responds to an input which is the sum of a signal and noise, both of which are considered stationary gaussian random processes with given power spectral density functions.
2. The desired output of the system is a function derived from the signal component of the input by some linear invariant operation, not necessarily physically realizable.
3. The criterion for optimality is minimum steady-state mean-squared error, which is the difference between the actual output of the system and the desired output.
4. The system contains an invariant stable linear part and a static single-valued nonlinear part which are considered fixed. The optimum linear, physically realizable compensation is to be designed for this system.

The system configuration is shown in Fig. 7.3-11.  $N$  and  $L(s)$  characterize the fixed nonlinear and linear parts of the system;  $G'(s)$  is the compensator to be designed. The original feedback configuration is recast in an open-chain configuration with a known relationship between the new cascade compensator  $G(s)$  and the original system compensator  $G'(s)$ . This is the configuration to which familiar filter theory is applicable were it not for the



nonlinear element in the chain. Using the theory of this chapter, the nonlinearity is characterized by its RIDF, which depends on  $\sigma_x$ . But the mean-squared value of  $x(t)$  is not known until  $G(s)$  is determined, and that depends on the gain of the nonlinearity. A logical way out of this dilemma is provided by the constrained optimum-design technique given by Newton, Gould, and Kaiser (Ref. 29). If a value is chosen for  $\sigma_x$ ,  $N_R$  is determined, and the constrained-optimum-design solution gives the function  $G(s)$  which minimizes the mean-squared error subject to the constraint that the mean-squared value of  $x(t)$  is as assumed. This solution is repeated for a number of values of the constrained variable  $\sigma_x^2$ . The mean-squared error corresponding to each of these is noted, and the solution which yields the smallest mean-squared error is optimum.

The solution to the constrained-optimum-design problem specialized to the configuration of Fig. 7.3-11 is given here for convenient reference. For the development of this solution, the reader is referred to Newton, Gould, and Kaiser (*op. cit.*).

With reference to Fig. 7.3-11, the quantity to be minimized is  $\overline{\epsilon(t)^2} + \lambda \overline{x(t)^2}$ , where  $\lambda$  is a Lagrange multiplier. We are considering unbiased variables in this section; so  $\overline{x(t)^2} = \sigma_x^2$ . The solution proceeds in the following steps:

1. Choose a value of  $\sigma_x$ . Calculate the corresponding value of  $N_R$  from

$$N_R = \frac{1}{\sqrt{2\pi}\sigma_x} \int_{-\infty}^{\infty} y(\sigma_x v) v \exp\left(-\frac{v^2}{2}\right) dv$$

2. Form the function

$$H(s) = N_R^2 L(s)L(-s) + \lambda$$

and factor it.

$$H(s) = H(s)_L H(s)_R$$

$H(s)_L$  contains all the factors of  $H(s)$  which define poles or zeros in the left half-plane, and  $H(s)_R$  contains all the factors of  $H(s)$  which define poles or zeros in the right half-plane. Any poles or zeros on the  $j\omega$  axis are moved just off the axis by the addition of a real part,  $\epsilon$ . For example, if  $H(s)$  has the factors  $1/(s)(-s)$ , they are replaced by  $1/(s + \epsilon)(-s + \epsilon)$ , the first factor becoming a factor of  $H(s)_L$  and the second a factor of  $H(s)_R$ .

3. Form the power spectral density functions  $[r(t) = s(t) + n(t)]$

$$\Phi_{rs}(s) = \Phi_{ss}(s) + \Phi_{ns}(s)$$

$$\Phi_{rr}(s) = \Phi_{ss}(s) + \Phi_{ns}(s) + \Phi_{sn}(s) + \Phi_{nn}(s)$$

and factor the input spectrum.

4. Form the function

$$M(s) = \frac{D(s)N_R L(-s)\Phi_{rs}(s)}{H(s)_R \Phi_{rr}(s)_R}$$

and separate it into

$$M(s) = M(s)_L + M(s)_R$$

where  $M(s)_L$  has its poles only in the left half-plane, and  $M(s)_R$  has its poles only in the right half-plane. The zeros of these functions may lie in either half-plane. This step is carried out by partial fraction expansion of  $M(s)$  and adding together those fractions which define poles in the left half-plane to form  $M(s)_L$ .  $M(s)_R$  need not be evaluated explicitly.

5. The optimum cascade compensation function is

$$G(s) = \frac{M(s)_L}{H(s)_L \Phi_{rr}(s)_L}$$

This is a function of the Lagrange multiplier  $\lambda$ .

6. Use the constraint condition

$$\sigma_x^2 = \frac{1}{2\pi j} \int_{-j\infty}^{j\infty} \Phi_{rr}(s) G(s) G(-s) ds$$

to evaluate  $\lambda$ , and hence  $G(s)$ , to yield the value of  $\sigma_x$  assumed in step 1.

7. Calculate the mean-squared error.

$$\begin{aligned} \bar{e}^2 &= \frac{1}{2\pi j} \int_{-j\infty}^{j\infty} \Phi_{ee}(s) ds \\ \Phi_{ee}(s) &= E(s)E(-s)\Phi_{ss}(s) + N_R^2 G(s)L(s)G(-s)L(-s)\Phi_{nn}(s) \\ &\quad + N_R G(s)L(s)E(-s)\Phi_{sn}(s) + N_R G(-s)L(-s)E(s)\Phi_{ns}(s) \\ E(s) &= N_R G(s)L(s) - D(s) \end{aligned}$$

The first two terms in this expression for the error power spectral density function are of the form of the integral tabulated in Table 7.3-1. The sum of the last two terms is also of this form.

This solution is repeated for enough values of  $\sigma_x$  to define a curve of  $\bar{e}^2$  versus  $\sigma_x$ . The value of  $\sigma_x$  which yields the minimum  $\bar{e}^2$  is then used in the final solution for the compensator  $G(s)$ . The solution to the problem of the design of the optimum linear compensation function for a nonlinear system of the form considered here is tedious, to be sure, but requires no new concepts and does provide a very satisfying solution to a rather



We might just note that describing function theory is applicable to systems with nonlinear parts separated by sufficient linear filtering regardless of what analytic form one chooses to describe the system. Time-variable systems or nonstationary system statistics are more conveniently treated with a *state space* characterization of the system than with a time-variable extension of integral transform theory. Under the assumption of known distribution for the components of a system state vector, the instantaneous nonlinearities involved in the system differential equation of state and in any nonlinear measurements taken on the system can be approximated as quasi-linear gain matrices using a multidimensional extension of Chap. 1 theory. In the case of a *non-limit-cycling nonlinear system driven by gaussian noise*, these gain matrices depend on the mean value and covariance matrix of the system state vector, and of any input noises. Having a quasi-linear description of the nonlinear system, linear filter theory in the form of the *Kalman filter* is employed directly to obtain approximate indications of the time-varying first- and second-order statistics of the system.

### OPTIMUM NONLINEAR COMPENSATION

A somewhat different problem is presented by a system having a given fixed part which is just asked to follow a random input as well as possible in the least-mean-squared-error sense. Consider any linear compensation to be fixed for simplicity in instrumentation. Then, for a given input spectrum, it is a simple matter to determine the optimum forward gain. Suppose now that we should like the system to respond optimally to inputs of various power levels; specifically, consider the shape and bandwidth of the input spectrum to remain fixed but scaled in amplitude to correspond to different rms input levels. For each input power level there will be a different optimum value of forward gain if the system fixed part contains a nonlinearity. What is needed, then, is a forward gain which depends on its input rms value, that is, a nonlinear element. If one permits some liberty in the application of RIDF theory, it is possible to design such a nonlinear compensator in an optimal way. The technique was first documented by Douce and King (Ref. 13).

The configuration of the system to be considered is shown in Fig. 7.3-12. The input signal is a stationary gaussian process with a power density spectrum which is of a prescribed shape but with a variable amplitude scaling. The fixed part includes the controlled member, its drive system, and any linear compensation which has been designed and is held fixed in this process. The nonlinearity  $N_1$  is to be designed to yield a minimum mean-

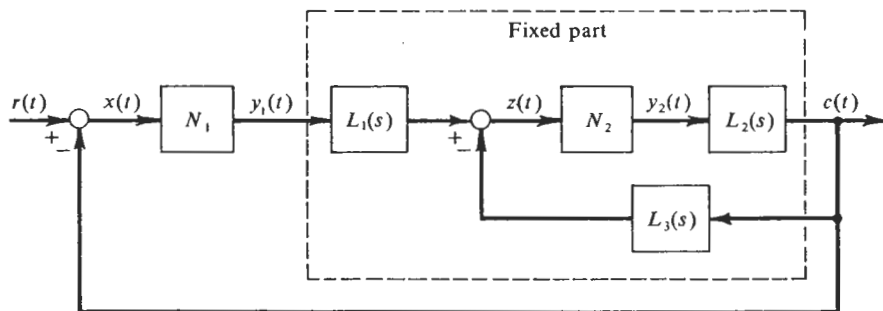


Figure 7.3-12 System configuration for design of optimum nonlinear compensation.

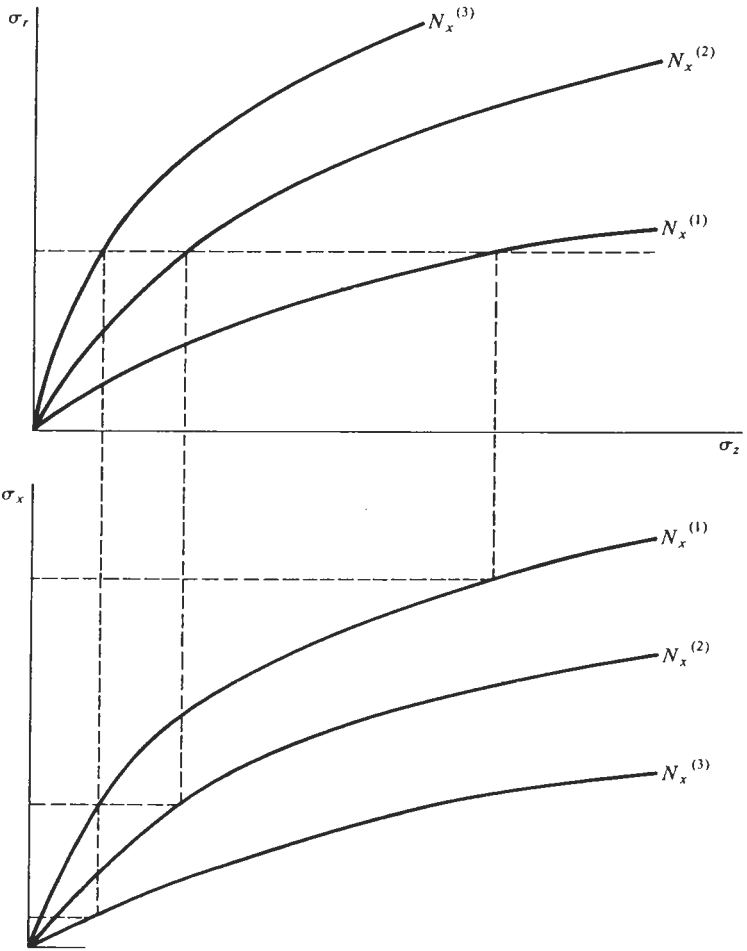
This may well imply a coarser degree of approximation than has been employed before in this section, since the output of the first nonlinearity is propagated to the input to the second without benefit of the heavy filtering of the controlled member. In some instances,  $L_1(s)$  may be unity or even a lead function; so the distribution of  $z(t)$  surely would not be normal, as assumed in the calculation of the RIDF for  $N_2$ . The only justification for proceeding is that the RIDFs for many nonlinearities, and in particular for the limiter which is of common interest in this context, are not strongly dependent on the distribution of the input. With the understanding that the accuracy of the approximation for  $N_2$  may not be up to the standard for RIDF usage, the solution proceeds in simple steps.

1. Choose a value for  $N_x$ , the RIDF for the unknown nonlinearity  $y_1(x)$ . Also choose a value for  $\sigma_z$ , and solve for the  $\sigma_r$  which results in this value of  $\sigma_z$ . This step is just like the "basic problem" discussed at the beginning of this section. Calculate the corresponding value of  $\sigma_x$ .
2. Repeat step 1 for enough values of  $N_x$  and  $\sigma_z$  to prepare plots of the form shown in Fig. 7.3-13.
3. At a given value of  $\sigma_r$ , use these plots to determine the value of  $\sigma_x$  corresponding to each choice of  $N_x$ . Plot these data for several values of  $\sigma_r$  as in Fig. 7.3-14.
4. For each input rms value there appears on these curves an optimum value of  $N_x$  (unless the solution is trivial). This is the value which minimizes the rms error. Cross-plot the optimum values of  $N_x$  against the corresponding values of  $\sigma_x$ , as shown in Fig. 7.3-14. This is the optimum RIDF for the nonlinearity  $y_1(x)$ .
5. Find a nonlinear function which has (nearly) the RIDF just determined.

In their illustrative example, Douce and King (Ref. 13) found that a nonlinearity of the form

$$y_1(x) = \begin{cases} ax^b & x \geq 0 \\ -y_1(-x) & x < 0 \end{cases}$$

with the proper choices of  $a$  and  $b$ , gave a suitable approximation to the required RIDF. The RIDF for this nonlinearity is given in Appendix E. Testing a simulation of the resulting system, Douce and King found the nonlinear compensator to reduce the system mean-squared error compared



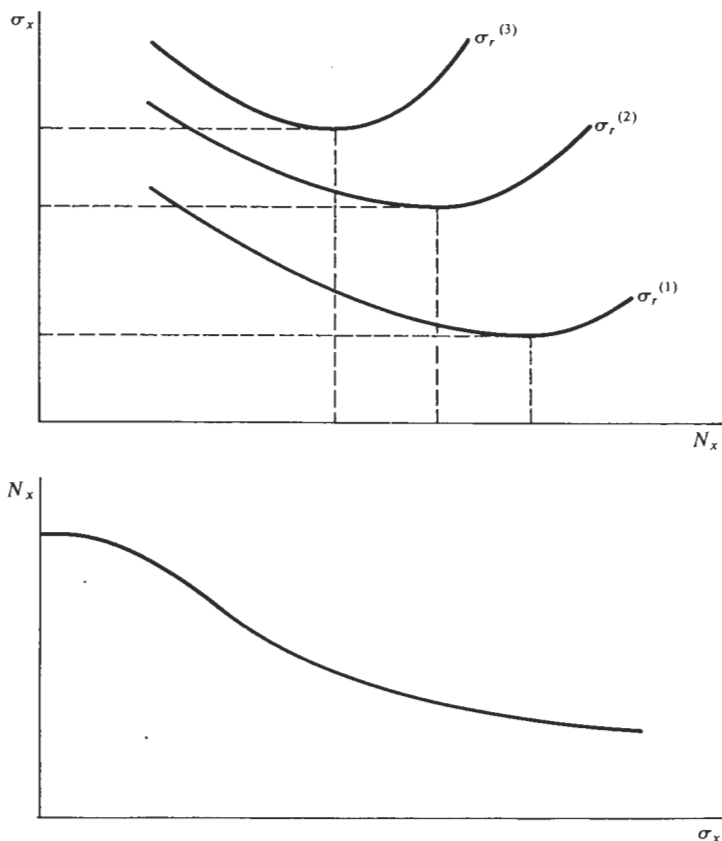


*Figure 7.3-14 Results of steps 3 and 4 of solution procedure for optimum nonlinear compensation.*

with the uncompensated nonlinear system by a factor which ranged up to 3:1 for some input conditions. Furthermore, the experimental results were in good agreement with the theoretical predictions, in spite of the fact that in their configuration there was no filter between  $N_1$  and  $N_2$ , as shown in Fig. 7.3-12.

#### 7.4 FEEDBACK SYSTEMS WITH RANDOM AND OTHER INPUTS

We now extend our attention to nonlinear systems having sinusoids and biases propagating around the loop, in addition to random processes. The class of problems which now lies within the range of our consideration is

truly impressive, and although the details of problem solution become more laborious with each step of increasing generality, the theory of multiple-input describing functions still provides practical answers to important questions that pertain to the design of real systems. It is now essential that one have the gains of the nonlinearity to the various components of its input calculated in advance, and perhaps plotted for ease of use. The RIDFs for several important nonlinearities are given in Appendix E; the methods of Sec. 7.2 can be used to calculate such data for others.

With these data at hand, it is a relatively simple matter to determine the effect of a random dither on a system limit cycle, to design the dither to meet a specification on limit cycle amplitude, or to calculate the amount of dither required to quench the limit cycle altogether. One can determine the characteristics of a noise input which will excite a limit cycle in a system which does not display one in the absence of input. The bandwidth and peak resonance of the sinusoidal response characteristic of a nonlinear system are altered by the addition of noise. It is possible to eliminate a jump resonance characteristic with noise. These phenomena are predictable within the present context. Systems with asymmetric nonlinearities can be considered, as well as systems with biased responses to inputs. For example, the average and mean-squared steady-state following error can be calculated for a limit cycling system responding to a ramp command and a random disturbance. Many other combinations of circumstances will give rise to the basic situation being considered in this section: a signal at the input to the system nonlinearity which is well modeled by the sum of a bias, a sinusoid, and a gaussian process.

#### USE OF RANDOM DITHER

Consider, first, the effect of a random noise, either intentionally supplied as a dither or otherwise appearing in a system, on the limit cycle and sinusoidal response characteristics of a system of the form shown in Fig. 7.3-1. If this system is excited by a gaussian process only, any sinusoid appearing at  $x(t)$  would have to be due to a limit cycle, and the performance of the system would be defined by the following relations:

$$N_A(A, \sigma_x) L_1 L_2 L_3(j\omega) = -1 \quad (7.4-1)$$

$$\sigma_x^2 = \frac{1}{2\pi j} \int_{-j\infty}^{j\infty} H(s) H(-s) \Phi_{rr}(s) ds \quad (7.4-2)$$

$$H(s) = \frac{L_1(s)}{1 + N_R(A, \sigma_x) L_1 L_2 L_3(s)} \quad (7.4-3)$$

These describing functions,  $N_A$  and  $N_R$ , pertain to the given nonlinearity driven by an input  $x(t)$ , which is modeled as the sum of a sinusoid and a gaussian process. No bias is being considered at the moment, which

implies an unbiased input to the system and an odd nonlinearity. The limit cycle condition [Eq. (7.4-1)] can be simplified in view of the basic restriction which has been observed throughout this chapter; namely, only static single-valued nonlinearities have been under consideration. Under this restriction, all the describing functions are real-valued static gains; so it is known in advance that if a limit cycle is to exist, all the required phase shift must be supplied by the linear part of the system. The limit cycle frequency, if any, is then the frequency at which the sinusoidal response function for the open-loop linear part of the system has  $180^\circ$  of phase lag. Call this frequency  $\omega_0$ . The amplitude of the open-loop linear sinusoidal response function at this frequency is known, and the complex Eq. (7.4-1) is reduced to the real equation

$$N_A(A, \sigma_x) = \frac{1}{|L_1 L_2 L_3(j\omega_0)|} \quad (7.4-4)$$

Equations (7.4-2) and (7.4-4) are now to be solved simultaneously for  $A$  and  $\sigma_x$  if the input spectrum  $\Phi_{rr}(s)$  is given. The solution defines the system limit cycle in the presence of the gaussian input and the input-output transfer characteristics of the limit cycling system to the gaussian input.

If the random input is applied as a dither for the purpose of controlling the amplitude of the limit cycle in the absence of other inputs, the dither may be applied either at the input or at some other station in the loop, such as directly at the input to the nonlinearity. Equations (7.4-4) and (7.4-2), with  $\Phi_{rr}(s)$  interpreted as the power density spectrum for the dither input, remain the same regardless of the point at which the dither is injected. In every case  $H(s)$  used in Eq. (7.4-2) is the closed-loop transfer function from the point where the dither is injected to the input to the nonlinearity, with the nonlinearity replaced by  $N_R$ . The *synthesis* problem of determining the amount of dither required to meet a specification on limit cycle amplitude is particularly simple to carry out. If  $A$  is specified and graphs of  $N_A$  and  $N_R$  as functions of  $A$  and  $\sigma$  are available, Eq. (7.4-4) can be solved immediately for  $\sigma_x$ . Then, with  $A$  and  $\sigma_x$  known, and if the shape of the power density spectrum of the random dither is chosen, Eq. (7.4-2) can be solved directly for the required rms value of the dither, no iterations or additional graphing being required. One caution must be observed, however. We shall see that nonlinear systems often display more than one mode of operation in their limit cycle behavior in the presence of random noise or dither. These modes correspond to multiple solutions to the equations defining the response. When a design is tentatively completed, the designer must check for the possibility of an additional solution; and if one exists, he must assure himself that the alternative limit cycle mode also meets the specification.

As an illustration of these procedures, Kwatny (Ref. 20) studied a system with a third-order linear part and an ideal-relay nonlinearity. The configuration is shown in Fig. 7.4-1. The input  $r(t)$  was a gaussian random

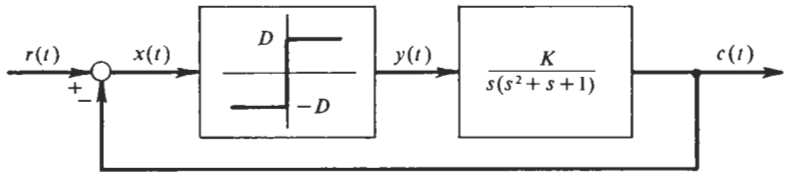


Figure 7.4-1 Kwatny's example system. (Ref. 20.)

process with power density spectrum

$$\Phi_{rr}(s) = \frac{2\tau\sigma_r^2}{1 - \tau^2s^2} \quad (7.4-5)$$

The RIDFs for the ideal relay with an input consisting of the sum of a gaussian process and a sinusoid are shown abbreviated from Appendix E in Fig. 7.4-2. We shall present the results for the case  $\sigma_r = 5$  units and  $\tau = 1$  sec with the gain of the system,  $KD$ , a parameter. For small values of this parameter no solution of Eq. (7.4-4) is possible. That is, for values of  $\sigma_x$  consistent with the given input and the low values of  $KD$ , there is no value of  $A$  for which  $N_A(A, \sigma_x)$  is large enough to satisfy Eq. (7.4-4). Over a range of gains, then, this system is predicted to display no limit cycle, although it is clear that it would limit-cycle for any gain if the noise were not present. The transfer of noise through the system in the absence of a limit cycle is described by Eq. (7.4-2), with  $N_R$  given by the  $A/\sigma = 0$  point in Fig. 7.4-2. For values of  $KD$  large enough to yield a solution to the limit cycle condition [Eq. (7.4-4)], there are in fact two solutions. Thus one predicts two possible modes of response: one with a relatively small  $A$  and large  $\sigma_x$ , the other with a relatively large  $A$  and small  $\sigma_x$ .

The theoretically predicted performance of this system is summarized in Fig. 7.4-3, which is a plot of the rms output of the system against system gain,  $KD$ , each normalized by the rms value of the input random process,  $\sigma_r$ . The mean-squared output, which is the only quantity that can conveniently be checked experimentally, includes both the transfer of noise to the output and the limit cycle at that point.

$$\overline{c(t)^2} = \frac{1}{2}A^2 + \text{mean-squared noise at } c$$

In the lower range of  $KD$ , there is just one mode of response with no limit cycle. The rms output is due entirely to the transfer of the input noise to  $c(t)$ . In the higher range of  $KD$ , the two solutions are shown with the limit cycle amplitude indicated along the two branches of the curve.

The actual performance of this system as observed in an analog simulation is entirely consistent with these predictions. Experimentally observed values of rms output are also shown on Fig. 7.4-3. In the region where no limit

cycle is predicted, the experimental and theoretical values of rms output differ by less than 10 percent. In the region where a limit cycle and two-mode operation are predicted, the observed rms output lies between the two theoretical values, suggesting an averaging between the two modes of operation. In his study of the actual output time histories, Kwatny (Ref. 20) observed the tendency to shift in a random manner between modes which would approximate those predicted. At the high end of the range of system gain, the tendency toward the larger-amplitude limit cycle mode was more pronounced.

In the case of a non-limit-cycling system, the gaussian-plus-sinusoid-input describing functions are useful in the study of the sinusoidal response characteristics of a nonlinear system with random noise or dither, or the random signal response characteristics of a nonlinear system with sinusoidal noise or dither. The noise transfer expression [Eq. (7.4-2)] is still applicable in this case, but the limit cycle condition [Eq. (7.4-4)] is replaced by the expression for the magnitude of the sinusoid response function of the closed-loop quasi-linearized system from system input to nonlinearity input.

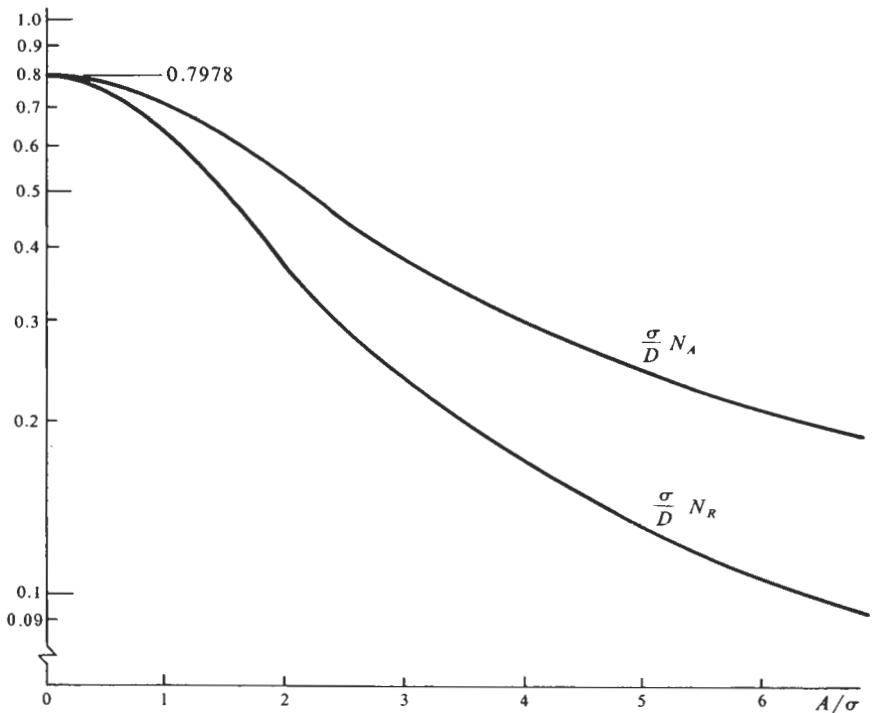


Figure 7.4-2 Gaussian-plus-sinusoid-input describing functions for the ideal-relay nonlinearity.



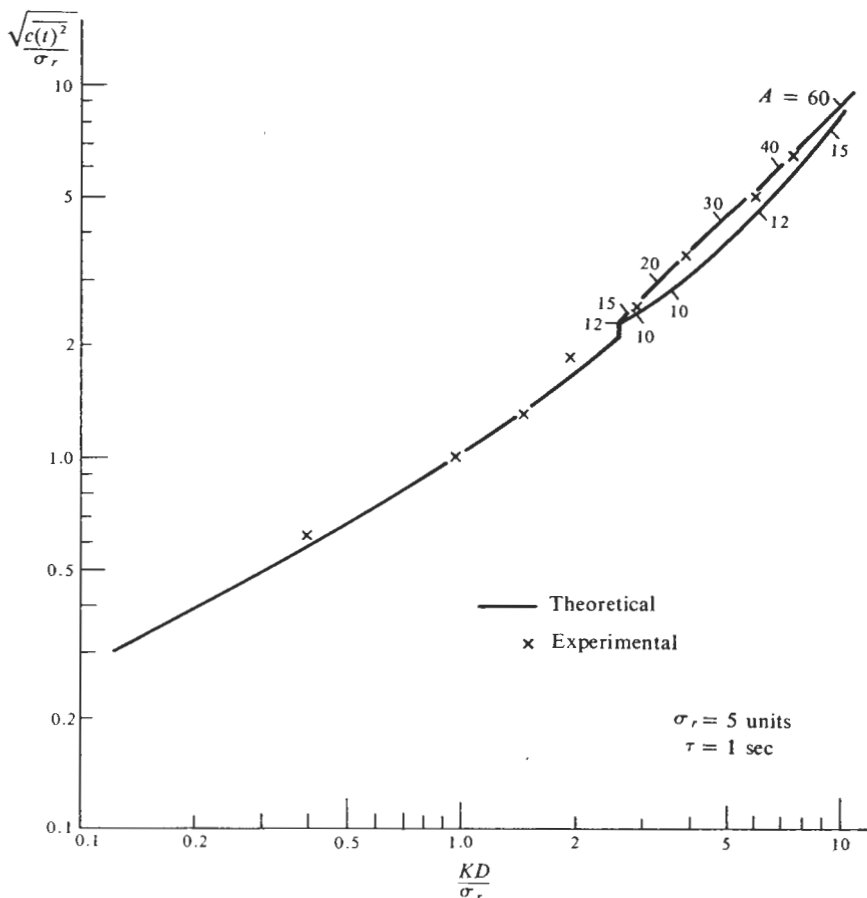


Figure 7.4-3 Performance of Kwatny's example system. (Adapted from Ref. 20.)

Nikiforuk and West (Ref. 31) show experimental results for the former in the case of a second-order system with a limiter nonlinearity. Their frequency response curves for different noise bandwidths or rms values show shifts in peak magnitude and in the frequency for peak magnitude which are completely understandable in terms of the decrease in the gain of the limiter to the sinusoid, with an increase in the rms noise at the input to the limiter. They also note that noise or random dither tended to quench the jump resonance in the frequency response characteristic. As the noise power was increased, the upper jump frequency tended to move down toward the lower until the jump phenomenon was eliminated.

These system characteristics, which are well explained by two-input RIDF theory, are difficult to think about qualitatively because of the complex

interrelation among  $N_A$ ,  $N_R$ ,  $A$ , and  $\sigma_x$ . The situation is considerably simplified if either  $A$  or  $\sigma_x$  can reasonably be treated as constant. This can be done in cases where the input sinusoid is very high frequency or the input noise is very wideband compared with the bandwidth of the quasi-linearized system. In such cases the system acts open-loop with respect to the high-frequency signal, since only a trivial amount is fed back. For example, if the input noise is wideband,  $\sigma_x$  can be determined once and for all, and the gain of the nonlinearity to the sinusoid is given by the curve of  $N_A$  versus  $A$  for the appropriate value of  $\sigma$ . From that point on, the problem is just like a single-sinusoid-input problem, but with a DF modified by the presence of the noise. The effect of the noise is invariably to "smooth out" the  $N_A$  curve, which is the qualitative explanation for the observed quenching of a jump resonance. The noise can either increase or decrease the gain of the nonlinearity to the sinusoid, depending on whether the slope of the nonlinearity generally increases or decreases with increasing input. For example, the presence of noise increases  $N_A$  in the case of a polynomial or hard-spring nonlinearity; it decreases  $N_A$  in the case of a soft-spring, limiter, or ideal-relay nonlinearity. Other nonlinearities have a combination of these effects. The relay with dead zone, for example, has a small slope (zero) for small signals, then a large slope (infinite), and then a small slope (zero) for large signals. Noise in this case increases  $N_A$  for  $A$  smaller than the dead zone, and decreases  $N_A$  for  $A$  much larger than the dead zone. Furthermore, the largest increase in  $N_A$  for small  $A$  is realized by an intermediate amount of noise such that  $\sigma_x$  is comparable with the dead zone.

Oldenburger and Sridhar (Refs. 33, 43) neglected the fed-back noise in their studies of random-signal stabilization. In the context of a more complete theory of quasi-linearization, this point of view is treated as an approximation which, when applicable, affords a significant simplification in problem solution. In view of the fact that the presence of noise can either increase or decrease the gain of the nonlinearity to a sinusoid, depending on the shape of the nonlinearity, it is easy to construct examples of systems in which noise will reduce or quench the limit cycle that would exist in the absence of input, and other examples in which noise will excite a limit cycle in a system which does not limit-cycle in the absence of input. The effect of the noise is very much like the effect of a second sinusoid in the system, and these examples are similar to the examples of sinusoidally quenched or excited limit cycles discussed in Sec. 5.4.

#### APPLICABILITY OF THE SINGLE-RANDOM-INPUT DESCRIBING FUNCTION

Use of the single-random-input describing function to study the response of a nonlinear system to a random input is always made under the same condition

as that required for use of the single-sinusoid-input describing function to study the response of a nonlinear system to a sinusoidal input, namely, that the system does not limit-cycle in the presence of the input. The two-sinusoid-input describing function is required to test for a limit cycle in the presence of an input sinusoid, and the gaussian-plus-sinusoid-input describing function is required to test for a limit cycle in the presence of a random input. The condition for the applicability of the single-random-input describing function was stated previously in the discussion of the use of dither: no limit cycle is indicated if for the  $\sigma_x$  corresponding to the given input and system configuration, there is no value of  $A$  for which  $N_A(A, \sigma_x)$  is as large as the reciprocal of the magnitude of the transfer function for the open-loop linear part at the frequency for  $180^\circ$  phase lag. This simply says that there is no solution to Eq. (7.4-4). This condition is simply stated; the difficulty in applying it is the determination of  $\sigma_x$ . A number of nonlinearities have the property that the maximum value of  $N_A(A, \sigma)$  as a function of  $A$  for a given  $\sigma$  occurs at  $A = 0$ . This is true, for example, of the ideal relay (see Fig. 7.4-2), the limiter, and soft-spring characteristics generally. In this case, the following point of view constitutes a most appealing pitfall: there can be no limit cycle if  $N_A(A, \sigma_x)$  for  $A = 0$  is less than  $1/|L(j\omega_0)|$ , where  $L(s)$  is the transfer function for the linear part of the system. But for  $A = 0$ ,  $\sigma_x$  can be determined using the simpler single-random-input describing function. Furthermore, it was shown previously [see Eq. (1.5-66)] that

$$\lim_{A \rightarrow 0} N_A(A, \sigma) = N_R(0, \sigma)$$

so the single-random-input describing function would seem to provide a check on its own applicability. The indicated procedure is to calculate  $\sigma_x$  using the single-random-input describing function; note that the corresponding  $N_R(\sigma)$  is equal to  $N_A(0, \sigma)$ , and see if this value is less than  $1/|L(j\omega_0)|$ . The more complicated gaussian-plus-sinusoid-input describing function need not be calculated at all, provided one is sure in advance that for any given  $\sigma$ ,  $N_A(A, \sigma)$  is never greater than  $N_A(0, \sigma)$ .

This argument, specialized to particular cases, was given by Kwatny (Ref. 20) and Gibson and Sridhar (Ref. 14), and in each case led to obviously incorrect results. The basic difficulty is the presence of *multiple solutions*; the user of describing function theory must always be alert to this possibility. The nature of the problem can be illustrated by reference to the system of Fig. 7.4-1. Suppose, first, that the rms input  $\sigma_r$  is taken as the variable parameter, and we wish to find the range of  $\sigma_r$  for which no limit cycle exists.  $1/|L(j\omega_0)|$  for this system is  $1/K$  and, for a specified  $K$ , is a known constant. The single-random-input describing function for the ideal relay is given by Eq. (7.2-31) with  $B = 0$ .

$$N_R(\sigma_x) = \sqrt{\frac{2}{\pi}} \frac{D}{\sigma_x} \quad (7.4-6)$$

According to the argument given above, we are looking for the range of  $\sigma_r$  which yields values of  $\sigma_x$  such that  $N_R(\sigma_x) < 1/K$ . But this is exactly the condition for stability of the system, with the nonlinearity replaced by the gain  $N_R$ . This interpretation of the condition for no limit cycle in terms of the stability of the quasi-linearized random-input-only system is not unique to this example; it is true of any system which is stable for all gains less than a critical value. However, all values of  $\sigma_r$  from zero to infinity yield stable systems in this example if random-noise-only theory is applied. This can be seen by noting that for large values of  $\sigma_r$ , the system cannot follow the input and  $\sigma_x$  tends toward  $\sigma_r$ . As  $\sigma_r$  is decreased,  $\sigma_x$  decreases, and thus  $N_R$  increases. As  $N_R$  approaches the value which would render the system unstable, corresponding to a known finite value of  $\sigma_x$ , the transfer of noise from  $r(t)$  to  $x(t)$  approaches infinity. Thus  $N_R$  approaching the critical value for stability corresponds to  $\sigma_r$  approaching zero. All positive values of  $\sigma_r$ , then, even vanishingly small values, yield values of  $N_R$  in the stable range, and the simplified limit cycle condition would say that no limit cycle exists since  $N_A(0, \sigma_x)$ , which is equal to  $N_R$ , is smaller than  $1/|L(j\omega_0)|$ . This does indeed constitute a solution to the mathematical problem, but it does violence to the physical problem. We know the no-input system limit cycles, and the limit cycle must persist for some range of small values of  $\sigma_r$ . If the theory is to be right, there must be another solution (or solutions) to the mathematical problem for small values of  $\sigma_r$ . The nature of the alternative solution can be seen by referring to the gaussian-plus-sinusoid-input describing functions of Fig. 7.4-2. If one admits the possibility of a limit cycle with  $A > 0$ , the effect of the sinusoid on  $N_R$  is to decrease it. For values of  $N_R$  close to the critical value for stability, a decrease in  $N_R$  means a decrease in  $\sigma_x$ . But the decrease in  $\sigma_x$  increases  $N_A$  to a value large enough to support the limit cycle. This alternative solution with  $A > 0$  defines the mode of operation we should expect to see in practice, and the solution can be found only by admitting the possibility of a limit cycle to the analysis.

A comparable situation exists if the input is fixed and the system gain  $KD$  is the variable parameter. If noise-only theory is used, all values of  $KD$  from zero to infinity are found to yield stable quasi-linearized systems, and in every case  $N_A(0, \sigma_x)$  is less than  $1/|L(j\omega_0)|$ . The nature of the solution as  $KD \rightarrow \infty$  is that  $\sigma_x$  goes to infinity (and thus  $N_R$  goes to zero) with  $KD$  in such a way that the quasi-linearized system just approaches the point of instability. However, for values of  $KD$  above one value, there are not only one, but two, additional solutions with nonzero values of  $A$ . As noted earlier, the actual system displays both of these modes.

In summary, there seems to be no reliable shortcut to the determination of the validity of random-input-only describing function theory. Except in the case of low-ordered systems which obviously cannot limit-cycle, the possibility of a limit cycle can be tested only by including a sinusoid in the analysis, and this requires full use of multiple-input describing function theory.

**A THREE-INPUT ILLUSTRATION**

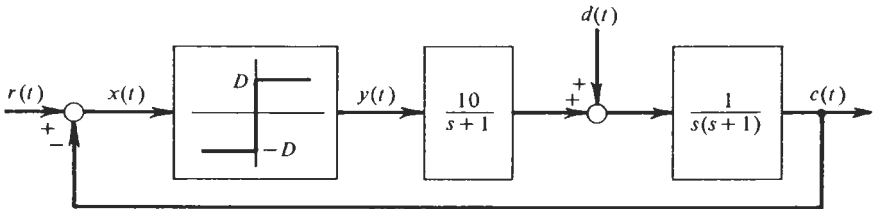
The presence of all three of the signal forms considered here at the input to the nonlinearity does not alter the nature of the analysis, only the labor required to apply it. The original nonlinear system is replaced by three quasi-linear systems, one to process each of the signal forms. In each of these quasi-linear systems, the nonlinearity is represented by the corresponding RIDF:  $N_B(A, B, \sigma)$ ,  $N_A(A, B, \sigma)$ , and  $N_R(A, B, \sigma)$ . The nonlinear character of the system is represented in the interdependence of these effective gains. The three quasi-linear systems yield three relations, one each for  $A$ ,  $B$ , and  $\sigma$ , in terms of the original system configuration and its inputs. These three expressions and the expressions for  $N_B$ ,  $N_A$ , and  $N_R$ , which will usually be represented by graphed data, must be solved simultaneously.

As an illustration of the recommended procedure, consider the system of Fig. 7.4-4. This system is responding to a ramp input  $r(t)$  and a gaussian disturbance  $d(t)$ . We wish to determine the mean value and standard deviation of the error in the steady state. The steady-state error response to the ramp is a constant due to the integration in the plant. In addition, it is clear that, for small enough disturbance inputs, the system will limit-cycle. Thus  $x(t)$  must be modeled as the sum of a bias, a sinusoid, and a random signal, and the three-input RIDFs must be employed. A sample of this nonlinearity input,  $x(t)$ , for particular choices of system parameters and input characteristics, is shown in Fig. 7.4-5. The bias in this signal is clearly evident, as is the limit cycle, and the irregularity of the record indicates the presence of the random noise.

The quasi-linear system which processes the bias signal has the same configuration as the original system, but the nonlinearity is replaced by  $N_B(A, B, \sigma)$ , and the only input is the ramp function  $r(t)$ . Because of the integration in the plant, the steady-state response of this quasi-linear system is evidently

$$10BN_B = k \tag{7.4-7}$$

The quasi-linear system which processes the sinusoid has the same configuration as the original system, but the nonlinearity is replaced by  $N_A(A, B, \sigma)$ ,



$$r(t) = kt$$

$$\Phi_{dd}(s) = \frac{2\tau\sigma_d^2}{1 - \tau^2s^2}$$

Figure 7.4-4 Three-input example system.

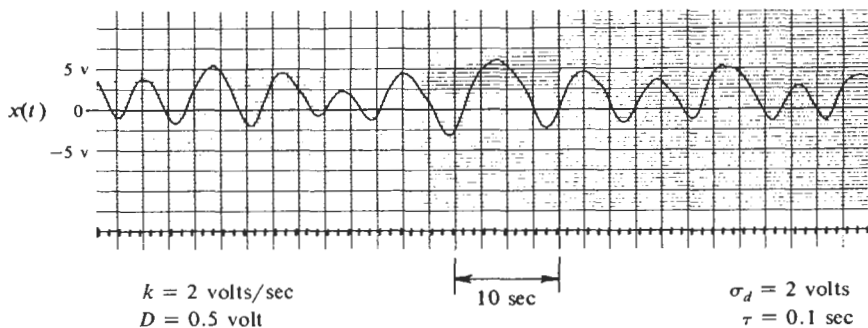


Figure 7.4-5 Sample of steady-state response. System of Fig. 7.4-4.

and there is no input. If this quasi-linear system is to display an undamped oscillatory mode corresponding to a limit cycle of the nonlinear system, the gain of the open-loop transfer function at the frequency for which it has  $180^\circ$  of phase lag must be unity. That frequency in this case is 1 radian/sec, and the limit cycle condition is

$$5N_A = 1 \quad (7.4-8)$$

The quasi-linear system which processes the random disturbance also has the same configuration as the original system, but the nonlinearity is replaced by  $N_R(A, B, \sigma)$ , and the only input is the gaussian disturbance  $d(t)$ . The  $\sigma$  which the three RIDFs depend on is the standard deviation of the random component of  $x(t)$ , the nonlinearity input. It is given by

$$\sigma^2 = \frac{1}{2\pi j} \int_{-j\infty}^{j\infty} \frac{2\tau\sigma_d^2}{1 - \tau^2 s^2} H(s)H(-s) ds \quad (7.4-9)$$

$$H(s) = -\frac{s+1}{s^3 + 2s^2 + s + 10N_R} \quad (7.4-10)$$

This integral can be evaluated using Table 7.3-1 to give an explicit expression for  $\sigma^2$  in terms of  $N_R$  and  $\sigma_d^2$  if  $\tau$  is given. This expression is

$$\sigma^2 = \sigma_d^2 \left[ \frac{\frac{10}{\tau} \left(2 + \frac{1}{\tau}\right) N_R + \left(2 + \frac{1}{\tau}\right) \left(1 + \frac{2}{\tau}\right) - \left(10N_R + \frac{1}{\tau}\right)}{10N_R \left[ \left(10N_R + \frac{1}{\tau}\right) \left(1 + \frac{2}{\tau}\right) \left(2 + \frac{1}{\tau}\right) - \frac{10}{\tau} N_R \left(2 + \frac{1}{\tau}\right)^2 - \left(10N_R + \frac{1}{\tau}\right)^2 \right]} \right] \quad (7.4-11)$$

The solution is most readily carried out by assuming a value for  $\sigma$ . Then, for each of the values of  $B/\sigma$  for which the describing functions are plotted in Appendix E, the value of  $A/\sigma$  which gives  $N_A = 0.2$  can be read from the graph, as well as the value of  $A/\sigma$  which gives  $BN_B = k/10$ . These sets of values are plotted versus  $B/\sigma$ , and the intersection indicates the values of  $A$  and  $B$  which result in satisfaction of Eqs. (7.4-7) and (7.4-8) for the chosen value of  $\sigma$ . This defines  $N_R$ , and Eq. (7.4-11) is solved for the value of  $\sigma_d^2$  which would result in the assumed value of  $\sigma$ . This procedure is repeated for several choices of  $\sigma$  to define the response of the system to a range of values of  $\sigma_d^2$ . One can then interpolate among these data to define the response for a given value of  $\sigma_d^2$ .

For some values of  $\sigma$  and  $B$  there will be no value of  $A$  for which  $N_A$  is as large as 0.2. This indicates no possibility of a limit cycle with those values of  $\sigma$  and  $B$ . For other choices of  $\sigma$  and  $B$  there may be more than one value of  $A$  for which the limit cycle condition can be satisfied. This indicates the possibility of multiple solutions, although one branch of such solutions may not be consistent with the requirement on gain to the bias. Another indication of multiple solutions can appear at the last step, where the relation between  $\sigma$  and  $\sigma_d$  may show more than one value of  $\sigma$ , and hence of  $A$  and  $B$ , corresponding to a single value of  $\sigma_d$ .

Having found  $A$ ,  $B$ , and  $\sigma$  for given ramp and disturbance inputs, the mean error is

$$\overline{x(t)} = B \quad (7.4-12)$$

and the standard deviation of the error is

$$\sigma_x = \sqrt{\sigma^2 + \frac{1}{2}A^2} \quad (7.4-13)$$

If multiple solutions are indicated, experience has shown that the actual system operation usually shifts randomly among the possible modes, and measured statistics represent some kind of average among the values of these statistics in the different modes.

## GENERALIZATION OF THE BIAS FUNCTION

The utility of multiple-input RIDFs is greatly broadened if one generalizes the bias which has been included as one of the characteristic forms of function at the input to the nonlinearity, allowing it to become an arbitrary function of time, within certain restrictions.

$$B \rightarrow B(t)$$

Within the necessary restrictions which must be placed on this extension of concept, one gains the tremendous advantage of being freed from the necessity of specifying in advance the form of each of the components of

signal at the nonlinearity input. Thus one can study, in a restricted sense to be sure, system stability, general transient responses, and other response characteristics that do not give rise to signal forms which can be known in advance.

The conditions under which the gain of a nonlinearity to a bias function,  $B$ , can reasonably be interpreted as the gain of that nonlinearity to an arbitrary function,  $B(t)$ , were discussed in Chap. 6 for the case in which  $B$ , or  $B(t)$ , appears at the nonlinearity input, together with a sinusoid. Our present consideration of this subject differs only in that random signals, as well, may be present. Although the presence of a random signal does not change the basic nature of this problem, it does complicate the writing of quantitative conditions under which the generalized interpretation of  $B$  is accurate. Qualitatively, one may say that if the nonlinearity input is observed over an interval long enough to include one period of the sinusoid and the interval of significant correlation of the random signal, the function  $B(t)$  should appear essentially constant. But more than this is involved. The gains of the nonlinearity to the sinusoid and to the random signal depend on  $B$ ; so if  $B$  changes, the system sinusoidal and random-signal response characteristics change. But we propose still to employ steady-state sinusoidal response characteristics and stationary (that is, steady-state) random response characteristics for the quasi-linearized system. So  $B(t)$  should also change slowly enough so that the system can be thought of as progressing through a continuous sequence of steady states as regards its sinusoidal and random response.

The generalization of  $B$  to  $B(t)$  can be justified, not only in the case where  $B(t)$  changes slowly enough, but also in the case where  $B(t)$  is small enough. For small enough  $B(t)$ ,  $N_A$  and  $N_R$  are little influenced by the changing  $B$ , and the system displays its steady-state sinusoidal and random responses. Moreover, we note from Eq. (1.5-63) that

$$\lim_{B \rightarrow 0} N_B = N_R(B = 0)$$

and from Eq. (1.5-66) that

$$\lim_{A \rightarrow 0} N_A = N_R(A = 0)$$

This says that the gain of a nonlinearity to a bias signal in the presence of any assortment of other signals is the same as the gain of that nonlinearity to a sinusoid in the presence of the other signals if both the bias and the sinusoid are small enough; and in fact this gain is the same as the gain of the nonlinearity to the random component of its input, which may be large or small. This suggests the thought that *the gain of the nonlinearity to a small signal in the presence of other signals is the same regardless of the shape of the small*



signal, and that this gain is the gain of the nonlinearity to the random component of input in the absence of the small signal. Just how small  $B(t)$  must be to qualify on the grounds of "smallness" rather than "slowness" cannot be stated in general; it depends on the nonlinearity. For those nonlinearities whose RIDFs are documented in Appendix E, the reader can see the range of  $B$  for which  $N_A$  and  $N_R$  are essentially independent of  $B$ , and  $N_B$  is nearly equal to  $N_R$ , and the range of  $A$  for which  $N_A$  is essentially equal to  $N_R$ .

The gain of the nonlinearity to small signals  $B(t)$  is just what is needed to study the stability of a system for small signals in the presence of others. The interesting kind of behavior which this allows one to test for is comparable with the case indicated in Chap. 6 of a system which has a stable limit cycle mode, but in the presence of that limit cycle the system is unstable for small signals. In this case we can consider a system which is responding to a random input and is also circulating one or more sinusoids which may result either from inputs or a limit cycle or both. In the presence of these signals, we wish to test the stability of the system to small signals. This test has a particularly simple interpretation when a random signal is present. For clarity, let us consider just one sinusoid. The stability of the system to small signals is given by the stability of the quasi-linearized system in which the nonlinearity is replaced by  $N_B(A, B, \sigma)$  with  $B = 0$ . The appropriate values of  $A$  and  $\sigma$  must be determined using the quasi-linearized system which propagates the sinusoid, in which the nonlinearity is replaced by  $N_A(A, B, \sigma)$  with  $B = 0$ , and the quasi-linearized system which propagates the random signal, in which the nonlinearity is replaced by  $N_R(A, B, \sigma)$  with  $B = 0$ . But once the simultaneous relations which define  $A$  and  $\sigma$  are solved, the stability to small signals is evident since

$$\lim_{B \rightarrow 0} N_B(A, B, \sigma) = N_R(A, 0, \sigma)$$

So if the quasi-linearized system which propagates the random signal is stable, the system is stable for arbitrary small signals in the presence of the random signal and sinusoid.

Popov (Ref. 35) solved this problem, taking a somewhat more complicated point of view. He considered a system with a bias and a random process and used the same gains as the describing functions  $N_B(B, \sigma)$  and  $N_R(B, \sigma)$  defined here to model the effect of the nonlinearity in transferring the bias and the random process. For the given random input to the system and for every arbitrary choice of  $B$ , the rms value of the random process at the nonlinearity input can be determined, using standard quasi-linear techniques. This gives a value of  $\sigma$  corresponding to every choice of  $B$ . Using this  $\sigma(B)$ , the gain to the bias function,  $N_B(B, \sigma)$ , is determined simply as a function of  $B$ . Now one can study a new nonlinear system in which the input to the

nonlinearity is  $B$  generalized to  $B(t)$  and the output is  $BN_B$ . This system has no random process appearing explicitly, but the effect of the random input to the original system is accounted for in the modification of the original nonlinearity to the new nonlinearity. For the study of the stability of the system in the presence of the random input, Popov uses small-signal linearization of the new nonlinearity about its origin. That is, he replaces the nonlinearity by a gain which is the slope of  $BN_B$  with respect to  $B$  at  $B = 0$ . But we now know, from Eq. (7.2-96), that

$$\frac{d}{dB}(BN_B) = N_R$$

so the gain derived in this way is exactly  $N_R(\sigma)$  for the value of  $\sigma$  corresponding to  $B = 0$ ! This procedure for the study of stability is then equivalent to the more direct approach described above.

A procedure similar to this can be employed to treat more complicated problems which depend on the assumption that the gain of the nonlinearity to a small or slowly varying signal  $B(t)$  is equal to the gain of the nonlinearity to a bias signal  $B$  in the presence of the same additional signals. Smith (Ref. 40) gives an example of the calculation of the transient response of a nonlinear system to a ramp input which is corrupted by an additive noise. The first part of the procedure is the determination of the equivalent nonlinearity for a noise-free system in which the effect of the noise in the original system is accounted for in the transformation of the original nonlinearity to the new nonlinearity. This is done as described above by considering the output of the new nonlinearity to be  $BN_B$ , in which the dependence upon  $\sigma$  has been eliminated by use of  $N_R(B, \sigma)$  to solve for the value of  $\sigma$  corresponding to each value of  $B$ . Having a new nonlinear system subjected to a noise-free ramp input, one can solve for the response in what seems to be the most convenient way. This is the most difficult step, since it may not admit of solution through quasi-linearization. We might note that if the problem were such that harmonic linearization of the new nonlinearity would lead to a solution, the result of the harmonic linearization of the new nonlinearity  $BN_B(B)$  would be exactly  $N_A(A, \sigma)$ , which might better have been calculated in the first place. Smith completed his example by treating the new nonlinearity as piecewise-linear in two ranges. This gives the mean response of the system to the noisy ramp input. This mean response has the interpretation that the response at every time is the mean, or average, of all possible responses at that time. It is thus the time-varying mean over the ensemble of responses to all possible inputs, each input consisting of the sum of the deterministic ramp function and a member of the ensemble of all possible noise functions. An estimate of probable deviations from this mean response can now be calculated by determining the noise transferred to the point where the response is measured, using  $N_R(B, \sigma)$  and the value of  $\sigma$  corresponding to each value of  $B$  in the mean response. If the response is being measured at

the input to the nonlinearity, this step is trivial, since the rms value of the noise at that point is already known as a function of  $B$ .

The system treated by Smith in his example is shown in Fig. 7.4-6. The mean response can be measured only by repeating the solution many times with random noise at the input and averaging over these responses at each point in time. Smith averaged over 25 recorded responses to determine the mean error response to the noisy ramp input. The results are shown in Fig. 7.4-7. Plotted in this figure are the theoretically computed mean error, the measured mean error at 0.1-sec intervals, and the 50 percent probable band for the distribution of the measured mean. Considering the fact that this calculation depends upon the approximations ordinarily involved in the application of describing function theory, and in addition uses stationary theory to process obviously nonstationary statistics, and uses the gain of the nonlinearity to the constant  $B$  as its gain to the slowly varying mean signal, the agreement seems quite good.

This use of RIDF analysis has little justification in theory. However, it does provide a means of attack on a very complicated class of problems—an attack which is both workable and somewhat satisfying physically.

## 7.5 ALTERNATE APPROACH FOR NONLINEARITIES WITH MEMORY

Throughout this chapter, attention has been restricted to static single-valued nonlinearities. This is not due to any limitation in the theory of multiple-input describing functions. The general describing function theory developed in Chap. 1 is valid for dynamic and multiple-valued nonlinearities as well, and in fact, application of the theory poses no great hurdle if nonlinearity inputs consisting of a bias and sinusoids only are considered. The difficulty with random inputs to a memory-type nonlinearity is purely a practical one: the optimum quasi-linear filter to pass the random input component is a dynamic filter in this case, and its determination requires solution of an

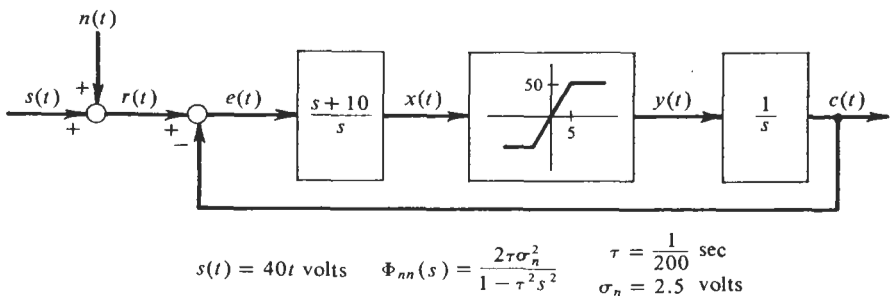


Figure 7.4-6 Smith's example system. (Ref. 40.)

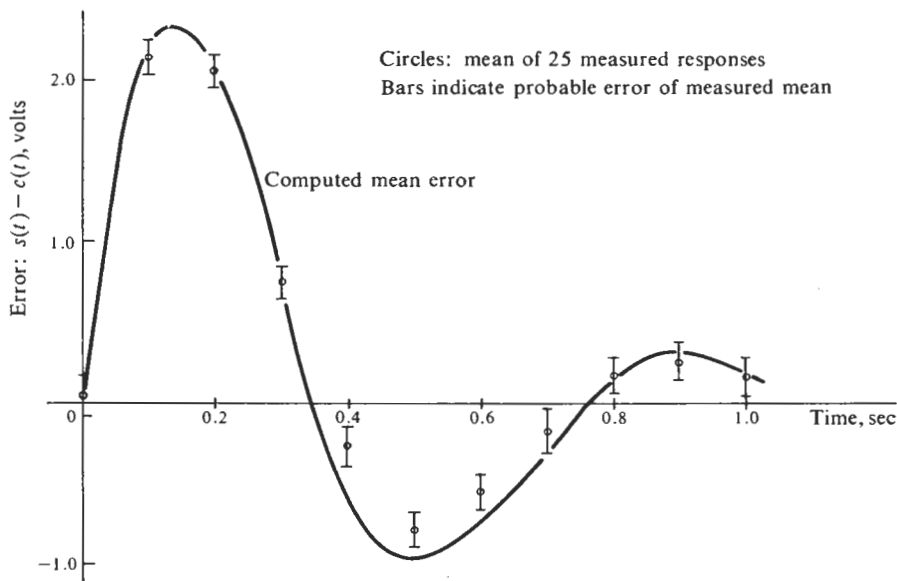


Figure 7.4-7 Results of Smith's example. (Ref. 40.)

integral equation of the Wiener-Hopf form [Eq. (1.5-44)]. The statistics which must be provided to effect the solution are the autocorrelation function for the random input and the cross correlation between the present output of the nonlinearity and all prior values of the random input. Just the evaluation of these statistics seems a forbidding chore, to say nothing of solving the integral equation. All this was found to simplify greatly in the case of static single-valued nonlinearities.

An entirely different approach to the determination of quasi-linear approximators to dynamic or multiple-valued nonlinearities with random inputs may be preferable. Because of the difficulty of calculating the distribution of random signals in dynamic nonlinear systems, we are constrained, as a practical matter, to assume the random signal appearing at the input to the nonlinearity to be gaussian. This assumption depends on the low-pass-filtering properties of the linear part of the system. But any gaussian random process can be expressed in the form of sinusoids: either as a sinusoidal function with random amplitude and phase or as the limit of a Fourier series with random coefficients (Ref. 38). With this description of the random input process, one can propagate the sinusoids representing the gaussian input, together with the actual sinusoidal input components and bias, through the nonlinearity, and identify the output components which are correlated with the input components. These relations, when averaged over the distributions of the random variables associated with the representation

of the input gaussian process, define the quasi-linear approximator based on the property of cross-correlation equivalence. These techniques are discussed by Levadi and Cosgriff (Ref. 24) and Mahalanabis and Nath (Ref. 25).

It may well be that the labor involved in quasi-linear approximation of dynamic and implicit nonlinearities enclosed in feedback systems renders the technique of little value in this case. The whole virtue of describing function analysis, as opposed, for example, to computer simulation of the system under study, is the understanding one gains of the system performance characteristics and the basis it provides for the rational design of systems. When the labor required to apply the technique exceeds some reasonable bound—and this bound depends strongly on each individual's facility in the technique—one's understanding of the system tends to be obscured, and the value of the analytic procedure in system design is decreased. This simply underscores the fact that we are dealing with very complicated problems. The impressive thing is the breadth of the range of complex and practically significant system situations in which quasi-linear techniques can be applied with reasonable facility.

## REFERENCES

1. Atherton, D. P.: The Evaluation of the Response of Single-valued Non-linearities to Several Inputs, *Proc. IEE*, vol. C-109, no. 15 (March, 1962), pp. 146-157.
2. Atherton, D. P.: Rapid Evaluation of the Auto-correlation Function of the Output of Single-valued Non-linearities in Response to Sinusoidal and Gaussian Signals, *Proc. IEE*, vol. C-109, no. 16 (September, 1962), pp. 656-664.
3. Axelby, G. S.: Random Noise with Bias Signals in Nonlinear Devices, *IRE Trans. Autom. Control*, vol. AC-4, no. 2 (November, 1959), pp. 167-172.
4. Barrett, J. F., and J. F. Coales: An Introduction to the Analysis of Non-linear Control Systems with Random Inputs, *Proc. IEE*, vol. C-103, no. 3 (November, 1955), pp. 190-199.
5. Booton, R. C., Jr.: Nonlinear Control Systems with Random Inputs, *IRE Trans. Circuit Theory*, vol. CT-1, no. 1 (March, 1954), pp. 9-17.
6. Booton, R. C., Jr., M. V. Mathews, and W. W. Seifert: Nonlinear Servomechanisms with Random Inputs, *MIT DACL Rept. 70*, August, 1953.
7. Burington, R. S.: "Handbook of Mathematical Tables and Formulas," 4th ed., McGraw-Hill Book Company, New York, 1964.
8. Caron J. Y.: Errors in the Quasi-linearization Technique for Nonlinear Systems, M.S. thesis, Massachusetts Institute of Technology, Department of Electrical Engineering, Cambridge, Mass., 1955.
9. Chuang, K., and L. F. Kazda: A Study of Nonlinear Systems with Random Inputs, *AIEE Trans.*, pt. II, vol. 78, no. 42 (May, 1959), pp. 100-105.
10. Culver, W. J., and M. D. Mesarovic: Dynamic Statistical Linearization, Joint Automatic Control Conference, paper 14-5, New York University, New York, 1962.
11. Davenport, W. B., Jr., and W. L. Root: "Introduction to Random Signals and Noise," McGraw-Hill Book Company, New York, 1958.
12. Douce, J. L.: A Note on the Evaluation of the Response of a Non-linear Element to

- Sinusoidal and Random Signals, *Proc. IEE*, vol. C-105, no. 7 (March, 1958), pp. 88-92.
13. Douce, J. L., and R. E. King: The Effect of an Additional Non-linearity on the Performance of Torque-limited Control Systems Subjected to Random Inputs, *Proc. IEE*, vol. C-107, no. 12 (September, 1960), pp. 190-197.
  14. Gibson, J. E., and R. Sridhar: The Response of Nonlinear Closed Loop Systems to Random Inputs, *Trans. ASME, J. Basic Eng.*, vol. D-86, no. 1 (March, 1964), pp. 132-138.
  15. Gusev, M. I.: Determining the Effect of Regular Signal Dynamics in the Statistical Linearization Method, *Automation and Remote Control*, vol. 21, no. 11 (May, 1961), pp. 1093-1100.
  16. Katkovnik, V. Y., and A. A. Pervozvanskii: Relay System with Self-oscillating Mode of Operation Disturbed by Random Signals, *Automation and Remote Control*, vol. 22, no. 5 (November, 1961), pp. 517-523.
  17. Kazakov, I. Y.: Approximate Probabilistic Analysis of the Operational Accuracy of Essentially Nonlinear Automatic Systems, *Automation and Remote Control*, vol. 17, no. 5 (1956), pp. 385-409.
  18. Kazakov, I. Y.: Problems of the Theory of Statistical Linearization and Its Applications, *Preprints of IFAC 1960 Moscow Confer.*, 1960, pp. 1968-1972, Butterworth Scientific Publications, London.
  19. Kislov, B. D.: Reduced Equivalent Amplification Factor of a Nonlinear Element in the Presence of Noise, *Automation and Remote Control*, vol. 21, no. 8 (March, 1961), pp. 804-809.
  20. Kwatny, H. G.: An Investigation of the Limit Cycle Characteristics of Nonlinear Systems in the Presence of a Random Noise, M.S. thesis, Massachusetts Institute of Technology, Department of Aeronautics and Astronautics, May, 1962.
  21. Laning, J. H., Jr., and R. H. Battin: "Random Processes in Automatic Control," McGraw-Hill Book Company, New York, 1956.
  22. Lee, Y. W.: "Statistical Theory of Communication," John Wiley & Sons, Inc., New York, 1960.
  23. Leland, H. R.: Input-Output Cross-correlation Functions for Some Memory-type Nonlinear Systems with Gaussian Inputs, *AIEE Trans.*, pt. II, vol. 79, no. 49 (July, 1960), pp. 219-223.
  24. Levadi, V. S., and R. L. Cosgriff: A Describing Function for Nonlinear Systems with Memory Subject to Random Input, *IEEE Trans.*, pt. II, *Appl. Ind.*, March, 1964, no. 71, pp. 73-76.
  25. Mahalanabis, A. K., and A. K. Nath: On the DIDFs of a Nonlinear Element with Memory, *IEEE Trans. Autom. Control*, vol. AC-11, no. 1 (January, 1966), pp. 138-139.
  26. Merchav, S. J.: Equivalent Gain of Single-valued Nonlinearities with Multiple Inputs, *IRE Trans. Autom. Control*, vol. AC-7, no. 5 (October, 1962), pp. 122-124.
  27. Merkulova, E. P.: The Problem of Optimizing Systems Which Contain Essentially Nonlinear Elements, *Automation and Remote Control*, vol. 20, no. 10 (June, 1960), pp. 1303-1313.
  28. Morosanov, I. S.: Effect of Fluctuations on Extremal Relay Systems under Self-oscillation Conditions, *Automation and Remote Control*, vol. 21, no. 9 (April, 1961), pp. 884-890.
  29. Newton, G. C., L. A. Gould, and J. F. Kaiser: "Analytic Design of Linear Feedback Controls," John Wiley & Sons, Inc., New York, 1957.
  30. Nikiforuk, P. N.: Response of a Particular Nonlinear Control System to Random Signals, *AIEE Trans.*, pt. II, vol. 75 (January, 1957), pp. 419-422.
  31. Nikiforuk, P. N., and J. C. West: The Describing Function Analysis of a Nonlinear Servo Mechanism Subject to Stochastic Signals and Noise, *Proc. IEE*, vol. C-104, no. 5 (March, 1957), pp. 193-203.

32. Nuttall, A. H.: Theory and Application of the Separable Class of Random Processes, *M.I.T. Res. Lab. Electronics, Tech. Rept.* 343, May, 1958.
33. Oldenburger, R., and R. Sridhar: Signal Stabilization of a Control System with Random Inputs, *AIEE Trans.*, pt. II, vol. 80, no. 57 (November, 1961), pp. 260-267.
34. Pastel, M. P.: Analyzing Nonlinear Systems with Random Inputs, *Control Eng.*, February, 1962, pp. 113-117.
35. Popov, E. P.: On Evaluating the Quality of Nonlinear Automatic Systems with Random Interference, *Automation and Remote Control*, vol. 20, no. 10 (June, 1960), pp. 1281-1287.
36. Pupkov, K. A.: Method of Investigating the Accuracy of Essentially Nonlinear Automatic Control Systems by Means of Equivalent Transfer Functions, *Automation and Remote Control*, vol. 21, no. 2 (October, 1960), pp. 126-139.
37. Pyatnitskii, G. I.: The Effect of Stationary Random Processes on Automatic Control Systems Containing Essentially Nonlinear Elements, *Automation and Remote Control*, vol. 21, no. 4 (November, 1960), pp. 328-332.
38. Rice, S. O.: "Mathematical Analysis of Random Noise," *Bell System Tech. J.*, vols. 23 and 24, 1944 and 1945. Reprinted in N. Wax, "Selected Papers in Noise and Stochastic Processes," Dover Publications, Inc., New York, 1954.
39. Sawaragi, Y., and S. Takahashi: Response of Control Systems Containing Zero-memory Non-linearity to Sinusoidal and Gaussian Inputs, *Proc. Heidelberg Conf. Autom. Control*, 1956, pp. 271-274.
40. Smith, H. W.: *Analysis of Nonlinear Feedback Systems with Random Inputs*, Sc.D. thesis, Massachusetts Institute of Technology, Department of Aeronautics and Astronautics, Cambridge, Mass., June, 1961. Revised as "Approximate Analysis of Randomly Excited Nonlinear Controls," Research Monograph 34, The M.I.T. Press, Cambridge, Mass., 1966.
41. Smith, H. W.: The Applicability of Quasi-linear Methods to Nonlinear Feedback Systems with Random Inputs, *Proc. Second IFAC Congr.*, Basel, Switzerland, August, 1963.
42. Somerville, M. J., and D. P. Atherton: Multi-gain Representation for a Single-valued Nonlinearity with Several Inputs and the Evaluation of Their Equivalent Gains by a Cursor Method, *Proc. IEE*, vol. C-105, no. 8 (July, 1958), pp. 537-549.
43. Sridhar, R., and R. Oldenburger: Stability of a Nonlinear Feedback System in the Presence of Gaussian Noise, *Trans. ASME, J. Basic Eng.*, March, 1962, pp. 61-70.
44. Thompson, W. E.: The Response of a Non-linear System to Random Noise, *Proc. IEE*, vol. C-102, no. 1 (September, 1954), pp. 46-48.
45. Tsympkin, Y. Z.: The Effect of Random Interference on a Periodic State in Relay Automatic Systems, *Soviet Phys.*, vol. 6, no. 7 (January, 1962), pp. 562-564.
46. Vander Velde, W. E.: A Nonlinear Method of Automatic Control in the Presence of Random Noise, Sc.D. thesis, Massachusetts Institute of Technology, Department of Aeronautical Engineering, May, 1956.
47. West, J. C., and P. N. Nikiforuk: The Response of Remote-position Control Systems with Hard-spring Non-linear Characteristics to Step Function and Random Inputs, *Proc. IEE*, vol. B-102, no. 5 (October, 1954), pp. 575-593.

## PROBLEMS

- 7-1. An alternative means of statistical linearization for static single-valued nonlinearities is to define an equivalent gain as the ratio of rms nonlinearity output to rms input. Consider the nonlinearity input to be an unbiased gaussian process, and compute this

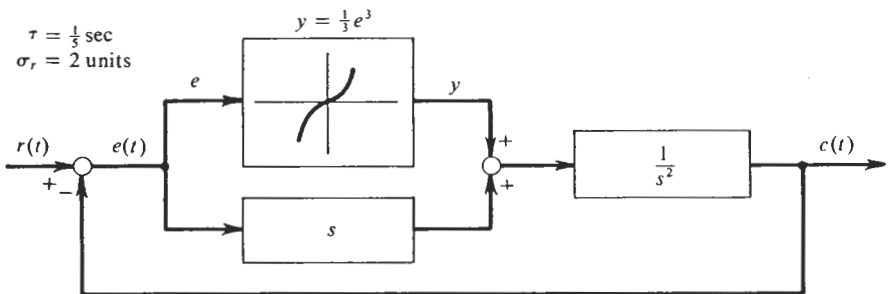
equivalent gain for the cubic nonlinearity, nonlinearity 18 of Appendix E. The integral form of Eq. (7.2-25) will be helpful in this calculation. Compare the result with  $N_R$  given in Appendix E.

- 7-2. Compute the rms equivalent gain for the relay with dead zone, nonlinearity 3 of Appendix E, and compare the result with  $N_R$  for a range of values of  $\sigma/\delta$ .
- 7-3. Compute the rms equivalent gain for the limiter, nonlinearity 7 of Appendix E, and compare the result with  $N_R$  for a range of values of  $\sigma/\delta$ .
- 7-4. Compute the gaussian-plus-bias-input RIDFs,  $N_R(\sigma, B)$  and  $N_B(\sigma, B)$ , for the piecewise-linear nonlinearity, nonlinearity 13 of Appendix E, using Eqs. (7.2-69) and (7.2-70) and the previously given expressions for  $I_1$  and  $I_2$ .
- 7-5. Note how  $N_R$  and  $N_B$  can be obtained for nonlinearities 3 to 5, 7 to 9, and 12 of Appendix E by specializing the results of Prob. 7-4.
- 7-6. Calculate  $N_R$  and  $N_B$  for nonlinearity 7 of Appendix E by specializing the results for nonlinearity 6.
- 7-7. Calculate  $N_R$  and  $N_B$  for nonlinearity 8 of Appendix E by writing the nonlinear function as the sum of a linear function plus nonlinearity 7. Note that this could also be done in the case of the three-input RIDFs, using the graphed data for the limiter.
- 7-8. Calculate  $N_R$  and  $N_B$  for nonlinearity 11 of Appendix E by specializing the results for nonlinearity 6, and by expressing the nonlinear function as the sum of two nonlinearities of the form of nonlinearity 8.
- 7-9. Calculate  $N_R$  and  $N_B$  for nonlinearity 13 of Appendix E by expressing the nonlinear function as the sum of a linear function plus nonlinearity 12, and by expressing it as the sum of nonlinear functions of the forms 3 and 9.
- 7-10. Calculate approximate values for the gaussian-plus-bias-input RIDFs for the limiter, nonlinearity 7 of Appendix E, for several choices of  $\sigma/\delta$  and  $B/\delta$ , using the integration formulas (7.2-85) and (7.2-86). Try both 10- and 20-point integration formulas, and compare the results with the analytic answers given in Appendix E.
- 7-11. Verify the relation

$$\frac{d}{dB}(BN_B) = N_R$$

in the case of the two nonlinearities for which analytic forms of the three-input RIDFs are given in Sec. E-3.

- 7-12. What is the steady-state mean-squared error in the system of Fig. 7-1 when driven by a gaussian process having the given power spectral density function?



$$\Phi_{rr}(s) = \frac{2\tau\sigma_r^2}{1 - \tau^2 s^2}$$

Figure 7-1



- 7-13. Using the results of Prob. 7-1, compute the theoretical value of  $\sigma_r$  corresponding to several choices of  $\sigma_x$  and  $a$  for which experimental points are plotted in Fig. 7.3-5. Compare these theoretical results, using the rms equivalent gain for the nonlinearity, with the experimental values and the theoretical results, using the describing function of this book (Fig. 7.3-5), and note that in almost every instance the describing function defined here gives more accurate results.
- 7-14. Do the same comparison as in Prob. 7-13, using the results of Prob. 7-2 and the data of Fig. 7.3-6.
- 7-15. Do the same comparison as in Prob. 7-13, using the results of Prob. 7-3 and the data of Fig. 7.3-7.
- 7-16. Determine the optimum linear compensator  $G'(s)$  and the resulting mean-squared error for the system of Fig. 7-2. The desired output is the signal component of the input.

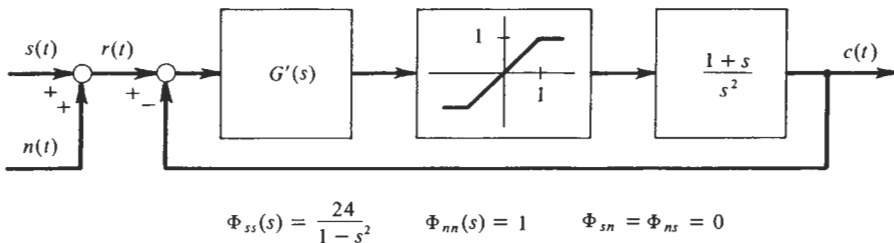


Figure 7-2

- 7-17. Determine the minimum rms value of gaussian dither,  $d(t)$ , which assures that the system of Fig. 7-3 will not limit-cycle in the absence of other inputs.

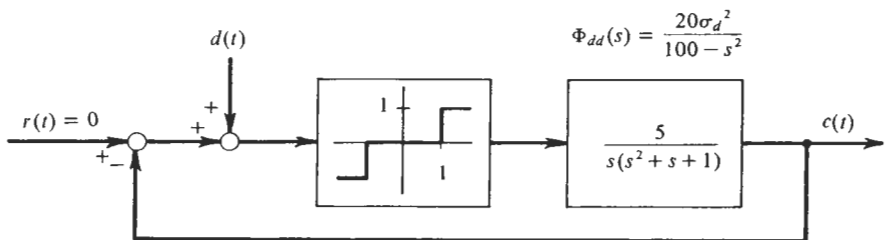


Figure 7-3

- 7-18. The system of Fig. 7-4 responds primarily to constant input commands and random disturbances. Plot the mean and standard deviation of the error,  $e(t)$ , for constant inputs ranging from 0 to 25 units.

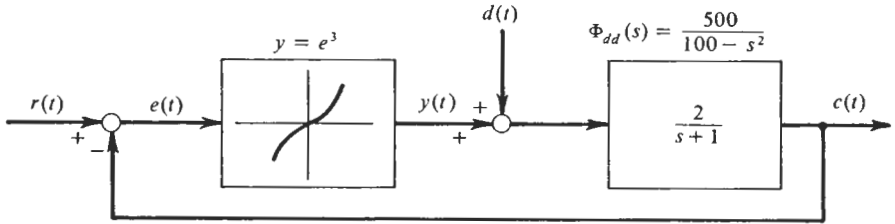


Figure 7-4

7-19. The system of Fig. 7-5 responds to a ramp command input and a gaussian disturbance input. What are the steady-state mean and variance of  $x(t)$  under the following conditions:

- $m = 2$  units/sec
- $D = 2$  units
- $K = 2 \text{ sec}^{-1}$
- $\Phi_{dd}(s) = 5 \text{ units}^2/\text{cps}$

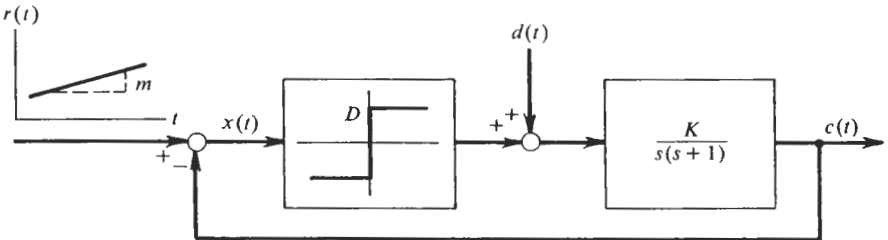
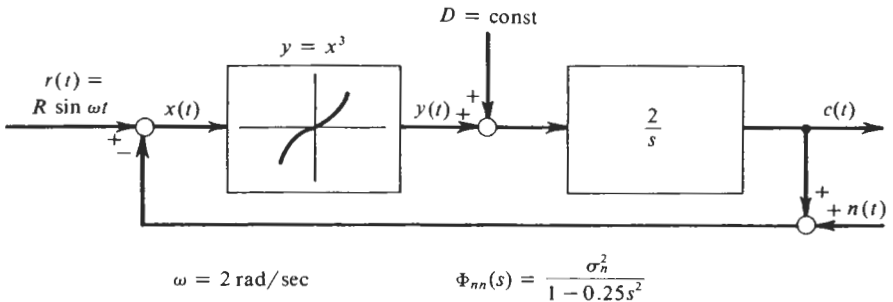


Figure 7-5

7-20. The system of Fig. 7-6 responds to a sinusoidal command input, a constant disturbance input, and a gaussian measurement noise in the feedback signal generator. What values of  $R$ ,  $D$ ,  $\sigma_n$  result in the error,  $x(t)$ , having a bias component of 1 unit, a sinusoidal component with amplitude 2 units, and a gaussian component with rms value of 1 unit?



$\omega = 2 \text{ rad/sec}$

$\Phi_{nn}(s) = \frac{\sigma_n^2}{1 - 0.25s^2}$

Figure 7-6

7-21. Solve the three-input illustration problem of Sec. 7.4 (system of Fig. 7.4-4) for the characteristics of the error,  $x(t)$ , in the case of the following parameter values:

$$k = 1 \text{ unit/sec}$$

$$D = 0.5 \text{ unit}$$

$$\tau = 0.1 \text{ sec}$$

$$\sigma_d = 1 \text{ unit}$$

7-22. Determine the modified nonlinearity for the system of Fig. 7.4-6 which accounts for the presence of noise in the system, and which can subsequently be used to evaluate the response to other inputs under the generalization of the bias signal to an arbitrary small or slow signal.